Theory of turbo machinery / Turbomaskinernas teori

Beyond Dixon

Computational Fluid Dynamics, CFD and Experimental methods

Det blir åttahundra grader. Du kan lita på mej. du kan lita på mej.
(Ebba Grön)

Background

Basic approachs (F.M. White)

1. Control Volume or large scale analyses
2. Differential analyses (NS-equations)
3. Experiments and/or dimensional analyses

CFD and experiments

- No, this is not a CFD course, but..
- Experiments

Background

Basic laws that can be used in Control Volume or Differential analyses

- Conservation of mass
- Conservation of linear momentum
- Conservation of angular momentum
- Conservation of energy

Computational Fluid Dynamics (CFD)

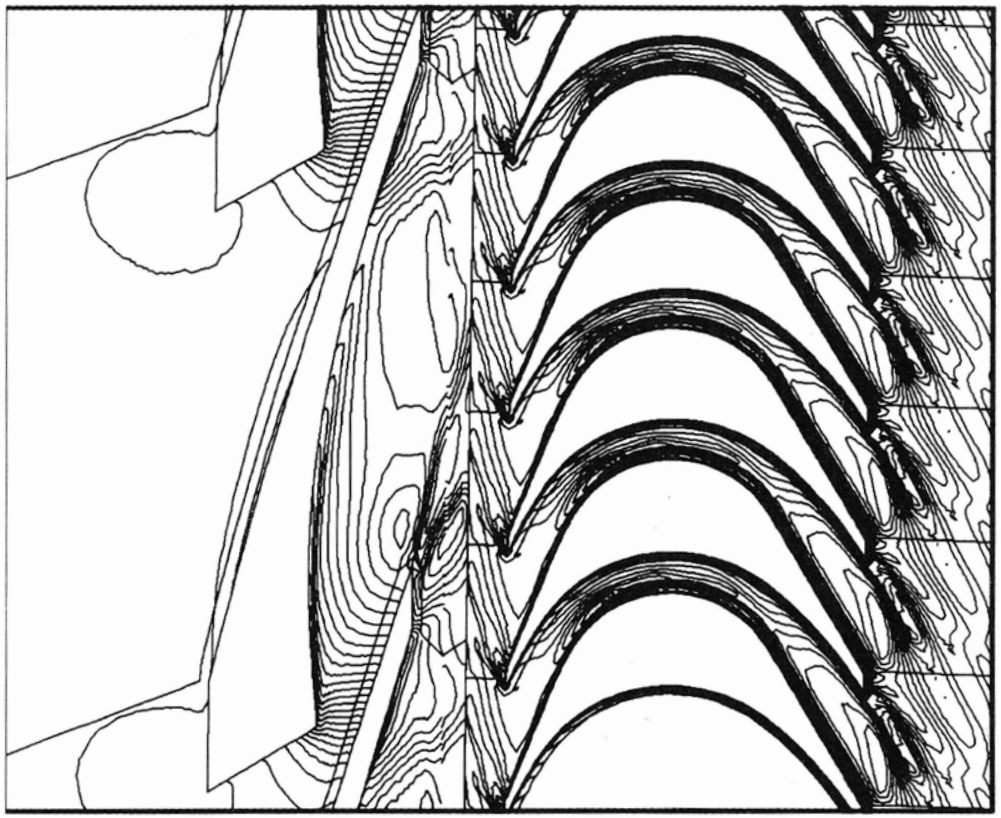

Fig 6 ISO-Mach number contours at mean radius.

U. Wåhlén, “The Aerodynamic design and testing of a supersonic turbine for rocket engine propulsion”, Proc. Of 3rd European conference on Turbomachinery: Fluid dynamics and thermodynamics

Computational Fluid Dynamics(CFD)

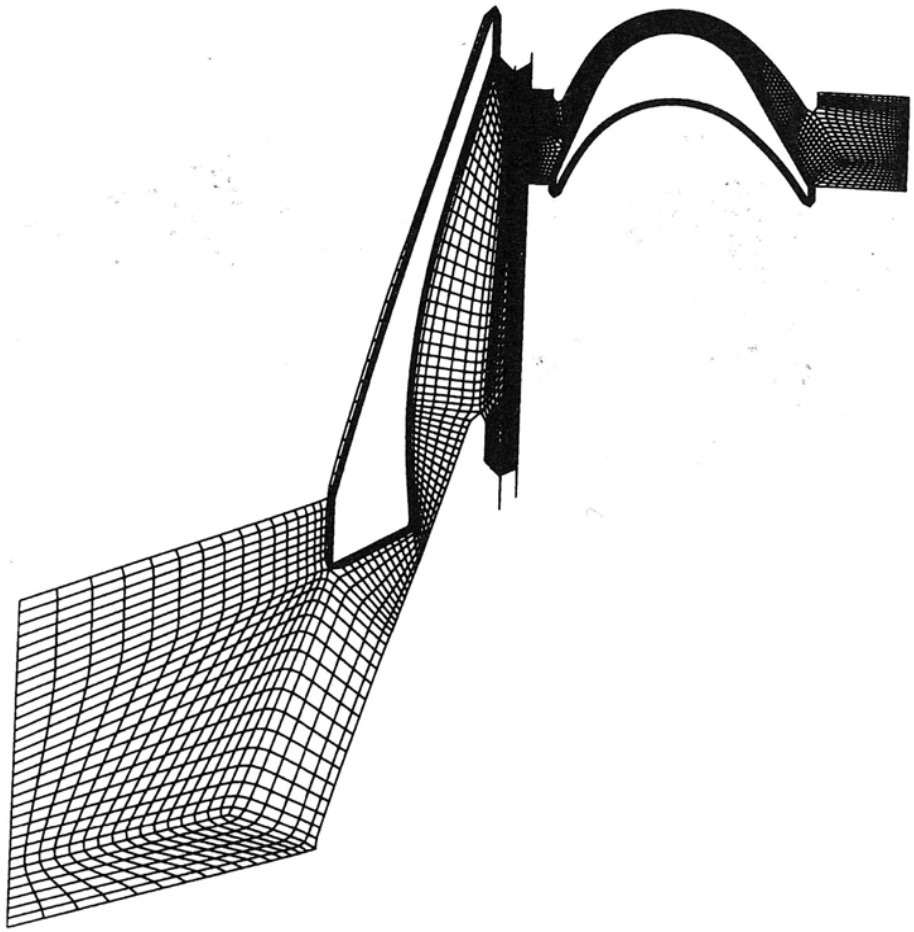

Fig 1 Turbine stator and rotor grid

Computational Fluid Dynamics(CFD)

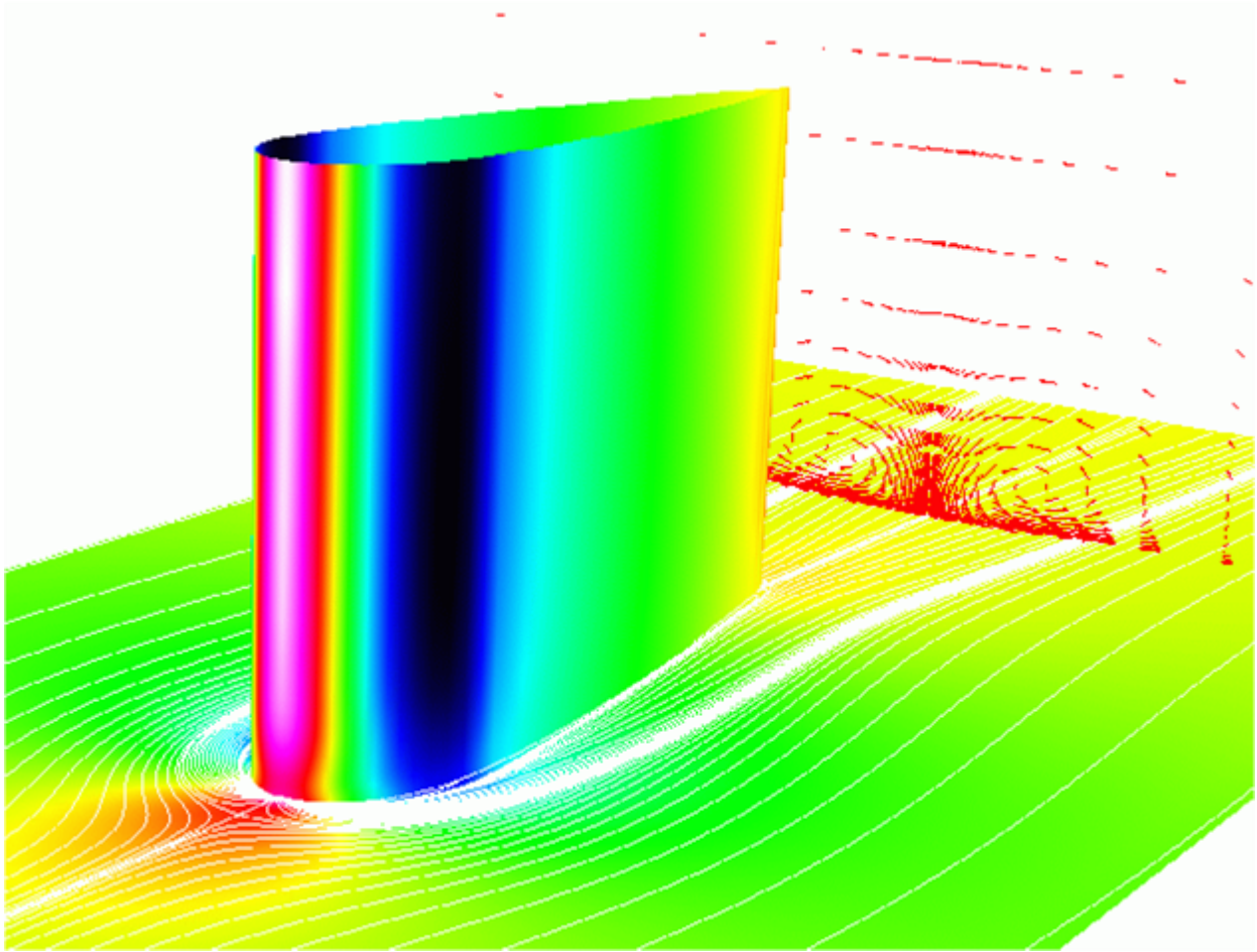

Subsonic flow in an aerofoil/plate junction computed with a second-moment closure (D. Apsley, 1998)

Computational Fluid Dynamics(CFD)

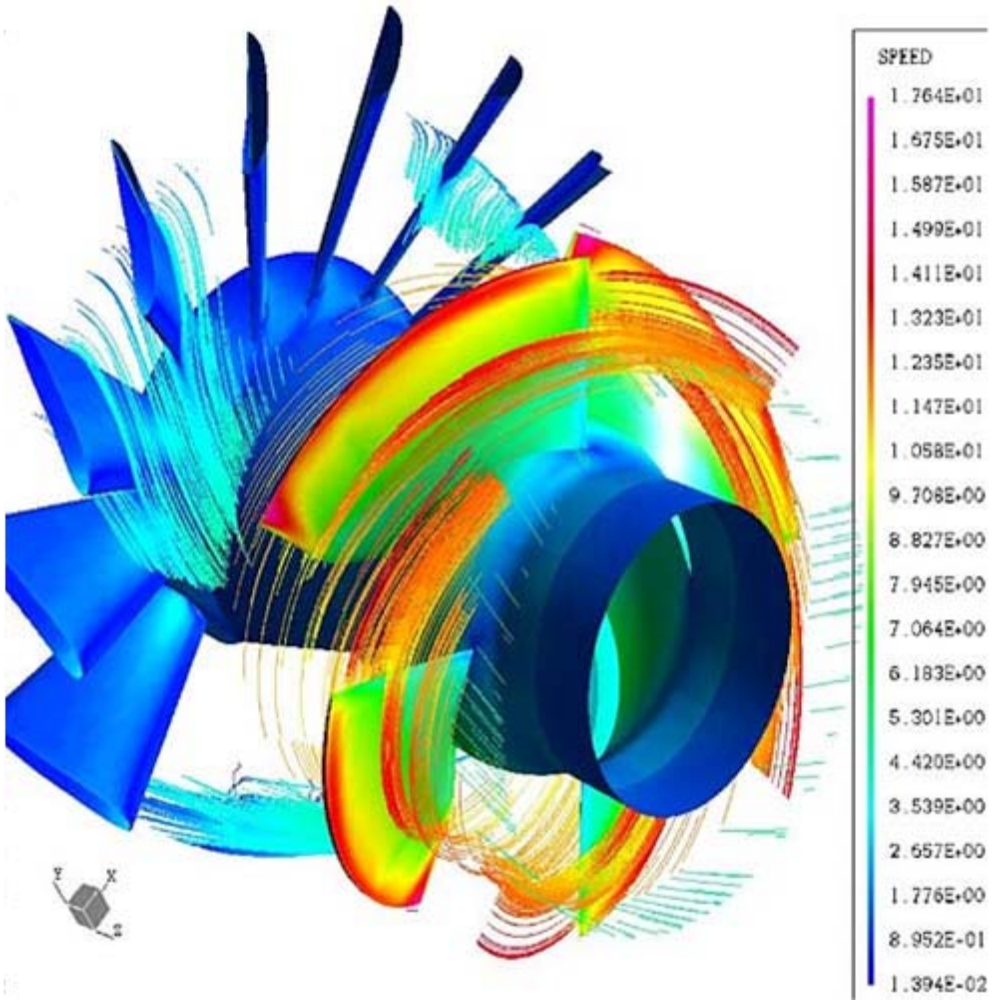

Hydraulic turbine research. CFD digital simulation.
Distribution of speed on an axial turbine

Computational Fluid Dynamics(CFD)

NS-Equations

Incompressible (isokor) stationary Navier-Stokes eq. and continuity eq: $\mathbf{u} = (u, v, w)$

$$\rho\left(u\frac{\partial u}{\partial x}+v\frac{\partial u}{\partial y}+w\frac{\partial u}{\partial z}\right)=-\frac{\partial p}{\partial x}+\left(\frac{\partial}{\partial x}\mu\frac{\partial u}{\partial x}+\frac{\partial}{\partial y}\mu\frac{\partial u}{\partial y}+\frac{\partial}{\partial z}\mu\frac{\partial u}{\partial z}\right)+\rho g_x$$

$$\rho\left(u\frac{\partial v}{\partial x}+v\frac{\partial v}{\partial y}+w\frac{\partial v}{\partial z}\right)=-\frac{\partial p}{\partial y}+\left(\frac{\partial}{\partial x}\mu\frac{\partial v}{\partial x}+\frac{\partial}{\partial y}\mu\frac{\partial v}{\partial y}+\frac{\partial}{\partial z}\mu\frac{\partial v}{\partial z}\right)+\rho g_y$$

$$\rho\left(u\frac{\partial w}{\partial x}+v\frac{\partial w}{\partial y}+w\frac{\partial w}{\partial z}\right)=-\frac{\partial p}{\partial z}+\left(\frac{\partial}{\partial x}\mu\frac{\partial w}{\partial x}+\frac{\partial}{\partial y}\mu\frac{\partial w}{\partial y}+\frac{\partial}{\partial z}\mu\frac{\partial w}{\partial z}\right)+\rho g_z$$

$$\frac{\partial u}{\partial x}+\frac{\partial v}{\partial y}+\frac{\partial w}{\partial z}=0$$

4 unknown (3 velocity components, pressure)
4 equations (3 NS eq. and continuity)

Nonlinear second order set of PDE
Only very simple analytic solution available

Turbulence is irregularity

- Small (unresolvable) scales
- Statistical approach required
- How can we define an average velocity?

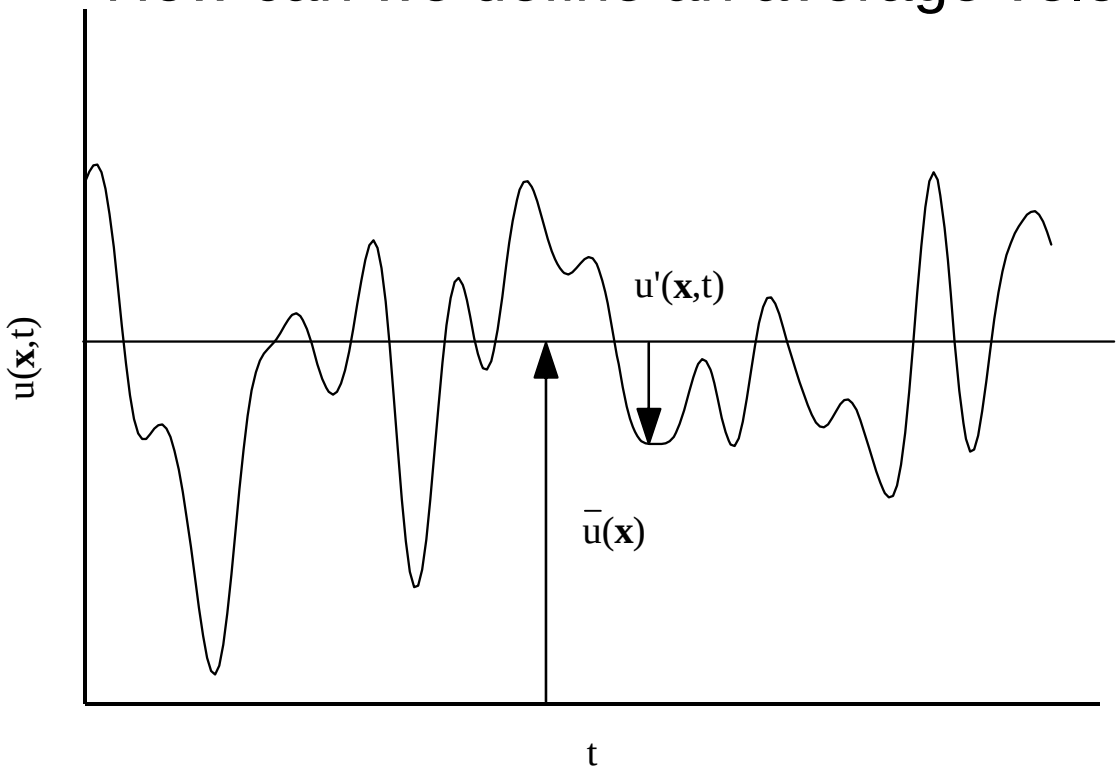

$$\bar{u}(\mathbf{x}) = \frac{1}{T}\int_0^T u(\mathbf{x},t)\,dt$$

Turbulence, averaging

Decompose velocity and pressure (Reynold's decomposition):

$$\mathbf{u} = \bar{\mathbf{u}} + \mathbf{u}' \qquad \text{and} \qquad p = \bar{p} + p'$$

Insert into NS and average entire equation (only axial equation shown):

$$\rho\left(\frac{\partial}{\partial x}\left(\bar{u}\,\bar{u}\right) + \frac{\partial}{\partial y}\left(\bar{u}\,\bar{v}\right) + \frac{\partial}{\partial z}\left(\bar{u}\,\bar{w}\right)\right) =$$

$$= -\frac{\partial \bar{p}}{\partial x} + \frac{\partial}{\partial x}\left(\mu\frac{\partial \bar{u}}{\partial x} - \rho\,\overline{u'u'}\right) + \frac{\partial}{\partial y}\left(\mu\frac{\partial \bar{u}}{\partial y} - \rho\,\overline{u'v'}\right) + \frac{\partial}{\partial z}\left(\mu\frac{\partial \bar{u}}{\partial z} - \rho\,\overline{u'w'}\right) + \rho g_x$$

Additional terms that look like stresses

Turbulence, RANS modelling

Reynolds stress tensor

$$\mathbf{R} = -\rho\,\mathbf{u}'\otimes\mathbf{u}' = R_{ij} = \rho\,\overline{u'_i\,u'_j} = \rho\begin{pmatrix} \overline{u'u'} & \overline{u'v'} & \overline{u'w'} \\ \overline{v'u'} & \overline{v'v'} & \overline{v'w'} \\ \overline{w'u'} & \overline{w'v'} & \overline{w'w'} \end{pmatrix}$$

Needs to be expressed as a function of variables we know or intend to solve for

TURBULENCE MODEL

Turbulence

10 unknown:
velocity components, pressure and correlations of fluctuating velocity, $\overline{u'v'}$

4 equations:
Averaged momentum equations and averaged continuity equation

Turbulence, RANS modelling

$$R_{ij} = \mu_T \left(\frac{\partial \bar{u}_i}{\partial x_j} + \frac{\partial \bar{u}_j}{\partial x_i} \right) - \frac{2}{3} \rho \, k \, \delta_{ij} \qquad \mu_T = \rho C_\mu k^2 / \varepsilon$$

$$\rho \bar{u}_k \frac{\partial k}{\partial x_k} = R_{kl} \frac{\partial \bar{u}_k}{\partial x_l} - \varepsilon + \frac{\partial}{\partial x_k} \left[\left(\mu + \frac{\mu_T}{\sigma_k} \right) \frac{\partial k}{\partial x_k} \right]$$

$$\rho \bar{u}_k \frac{\partial \varepsilon}{\partial x_k} = C_{\varepsilon 1} \frac{\varepsilon}{k} R_{kl} \frac{\partial \bar{u}_k}{\partial x_l} - \rho C_{\varepsilon 2} \frac{\varepsilon^2}{k} + \frac{\partial}{\partial x_k} \left[\left(\mu + \frac{\mu_T}{\sigma_\varepsilon} \right) \frac{\partial \varepsilon}{\partial x_k} \right]$$

Closure coefficients

$C_{\varepsilon 1} = 1.44 \qquad C_{\varepsilon 2} = 1.92 \qquad C_\mu = 0.09 \qquad \sigma_\varepsilon = 1.3 \qquad \sigma_k = 1$

References, turbulence

- **Tennekeys and Lumley, *“A first course in Turbulence”*, MIT Press, 1972.**
- **J. O. Hinze, *“Turbulence”*, McGraw-Hill, 1959.**
- **D. C. Wilcox, *“Turbulence Modeling for CFD”*, DCW Industries, 1998.**

CFD and experiments

- No, this is not a CFD course, but..
- **Experiments**

What do we need to measure?

Overall performance

- Flow rates (mass or volume)
- Pressure
- Temperature
- Shaft power

Performance increase

- Separations (velocity)
- Secondary flows, e.g. tip clearance losses (velocity)
- Shock waves (supersonic applications)
- Pressure (resolved in time and space)
- Temperature (resolved in time and space)

Cascade wind tunnels

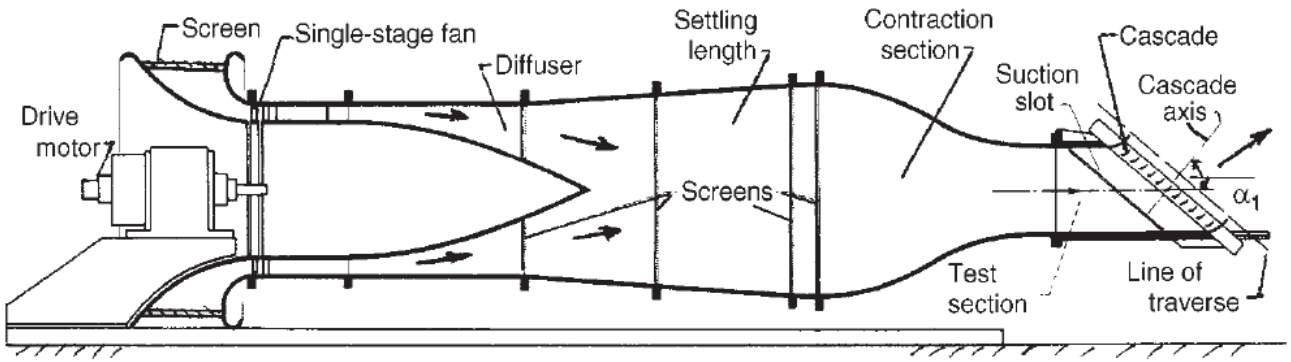

(a)

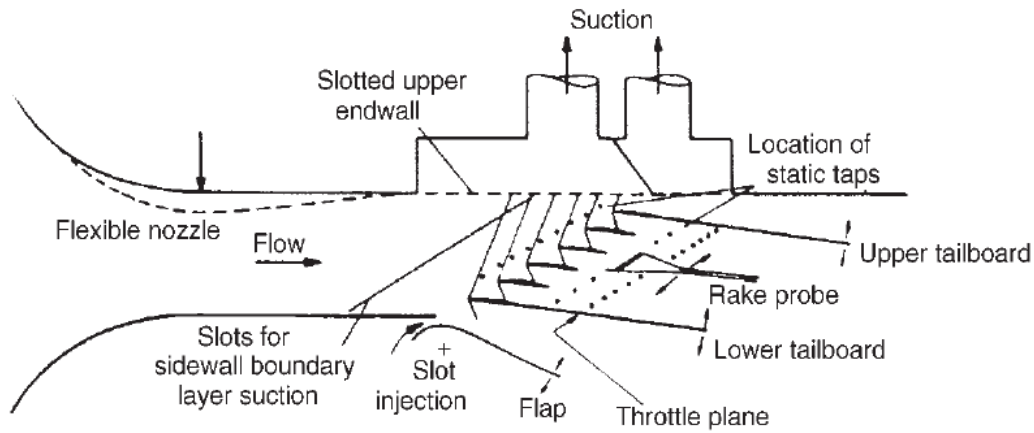

(b)

FIG. 3.1. Compressor cascade wind tunnels.
(a) Conventional low-speed, continuous
running cascade tunnel (adapted from Carter et al. 1950).
(b) Transonic/supersonic cascade tunnel (adapted from Sieverding 1985).

Closed circuit tunnels

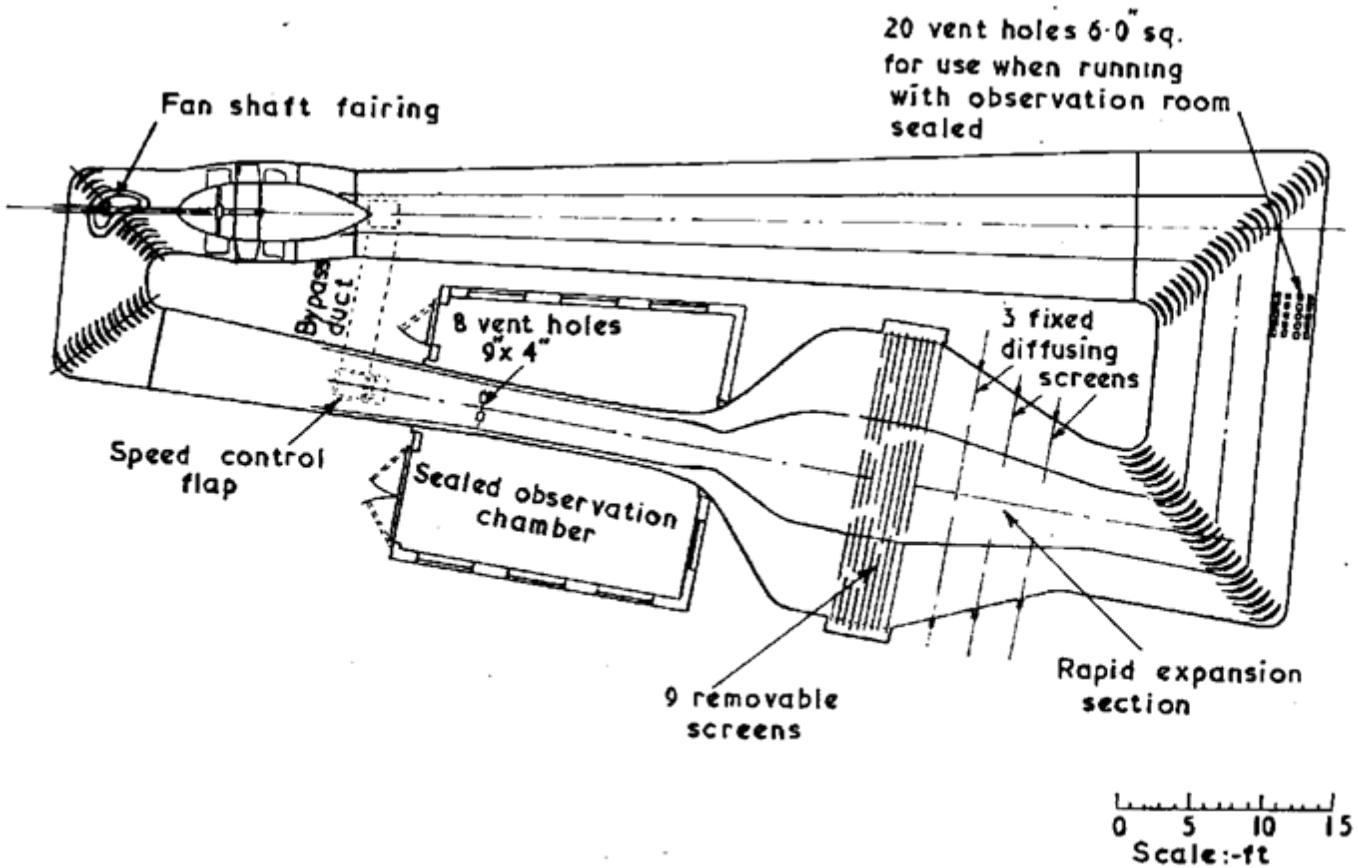

RAE 4 ft × 3 ft wind tunnel (1946).

components

Settling Chamber

The settling chamber is located between the fan or wide angle diffuser and the contraction and contains the honeycombs and screens used to moderate longitudinal variations in the flow. Screens in the chamber should be spaced at 0.2 chamber diameters apart so that flow disturbed by the first screen can settle before it encounters the second.

Honeycombs

Honeycombs are located in the settling chamber and are used to reduce nonuniformities in the flow. For optimum benefit, honeycombs should be 6-8 cell diameters thick and cell size should be on the order of about 150 cells per settling chamber diameter.

components

Screens

Screens are typically located just downstream of the honeycomb and sometime at the inlet of the test section. Screens create a static pressure drop and serve to reduce boundary layer size and increase flow uniformity.

Contraction Section

Contractions sections are located between the settling chamber and the test sections and serve to both increase mean velocities at the test section inlet and moderate inconsistencies in the uniformity of the flow. Large contraction ratios and short contraction lengths are generally more desirable as they reduce the power loss across the screens and the thickness of boundary layers. Small tunnels typically have contraction ratios between 6 and 9.

Flow meters with pressure measurement

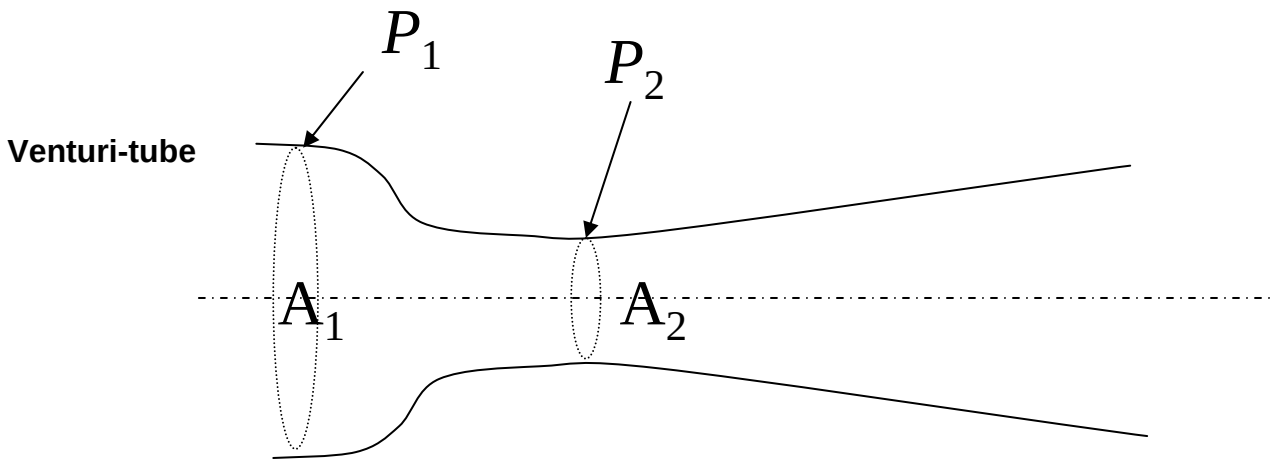

In the incompressible case $C_1 A_1 = C_2 A_2$

Assuming horisontal mounting $\frac{C_1^2}{2} + \frac{P_1}{\rho} = \frac{C_2^2}{2} + \frac{P_2}{\rho}$

Daniel Bernoulli 1700-1782

Daniel Bernoulli was the son of Johann Bernoulli. He was born in Groningen while his father held the chair of mathematics there. His older brother was Nicolaus(II) Bernoulli and his uncle was Jacob Bernoulli so he was born into a family of leading mathematicians but also into a family where there was unfortunate rivalry, jealousy and bitterness.

Undoubtedly the most important work which Daniel Bernoulli did was his work on hydrodynamics. Even the term itself is based on the title of the work which he produced called Hydrodynamica and, before he left St Petersburg, Daniel left a draft copy of the book with a printer. However the work was not published until 1738 and although he revised it considerably between 1734 and 1738, it is more the presentation that he changed rather then the substance.

This work contains for the first time the correct analysis of water flowing from a hole in a container. This was based on the principle of conservation of energy which he had studied with his father in 1720. Daniel also discussed pumps and other machines to raise water. One remarkable discovery appears in Chapter 10 of Hydrodynamica where Daniel discussed the basis for the kinetic theory of gases. He was able to give the basic laws for the theory of gases and gave, although not in full detail, the equation of state discovered by Van der Waals a century later.

Flow meters with pressure measurement

Venturi-tube (2)

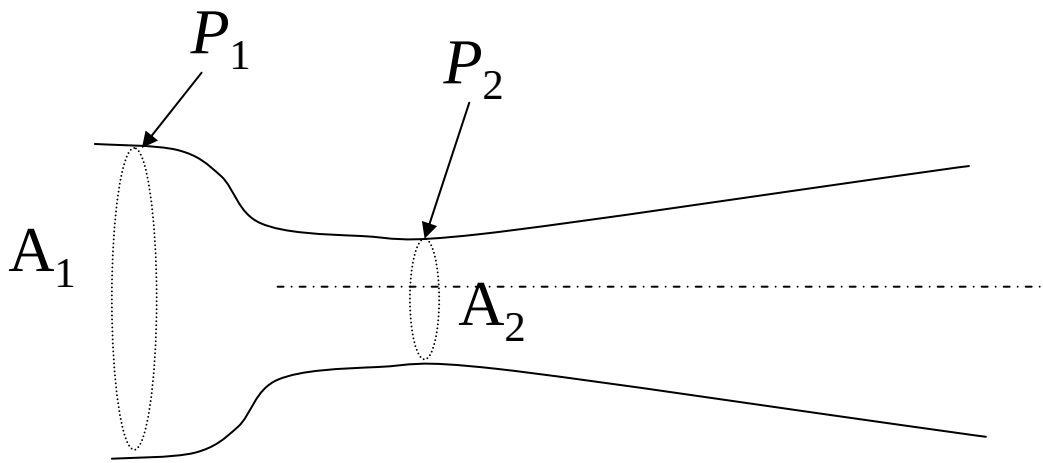

Solve for e.g. c_2:

$$C_2^2 - C_2^2 \left(\frac{A_1}{A_2} \right)^2 = \frac{2\Delta P}{\rho}$$

where $\Delta P = P_1 - P_2$

$$C_2 = \left(\frac{2\Delta P}{\rho\left(1 - A_1^2 / A_2^2\right)} \right)^{1/2}$$

and $$\dot{m} = \rho A_2 C_2 = A_2 \left(\frac{2\rho\Delta P}{\left(1 - A_1^2 / A_2^2\right)} \right)^{1/2}$$

Flow meters with pressure measurement

Orifice meters

- Applicable for pipe flows
- Same principle as for Venturi
- Positioning of pressure taps important
- Vena contracta and losses require inclusion of Discharge Coefficient, C_D

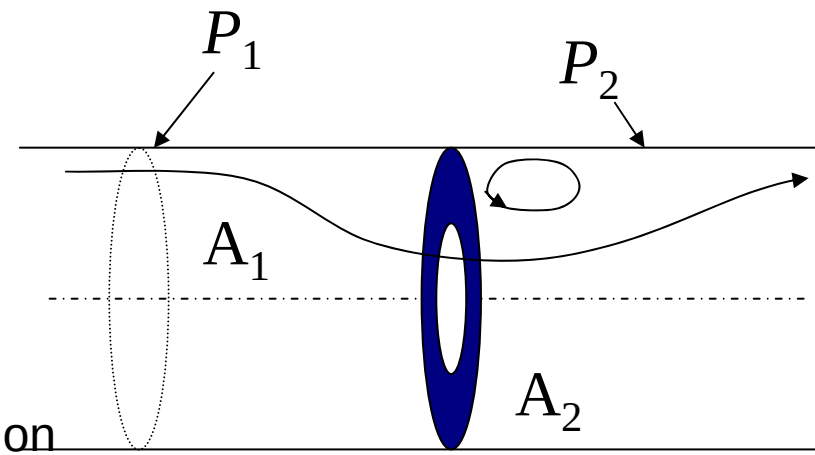

$$\dot{m} = C_D A_2 \left(\frac{2\rho \Delta P}{\left(1 - A_1^2 / A_2^2\right)} \right)^{1/2} \qquad \text{where} \qquad C_D = f\left(\mathrm{Re}, A_1/A_2\right)$$

C_D available from manufacturer (measurements) or Standards (e.g. ISO)

Coriolis flow meter

An actuator (not shown) induces a vibration of the tubes

When there is mass flow, Coriolis forces induce twisting of the tubes

degree of phase-shift is a measure for the amount of mass that is flowing through the tubes

Thermal flow meter

- Heat is added electrically to the flow
- Temperature is measured before and after heat addition

$$P = \dot{m} C_p \Delta T$$

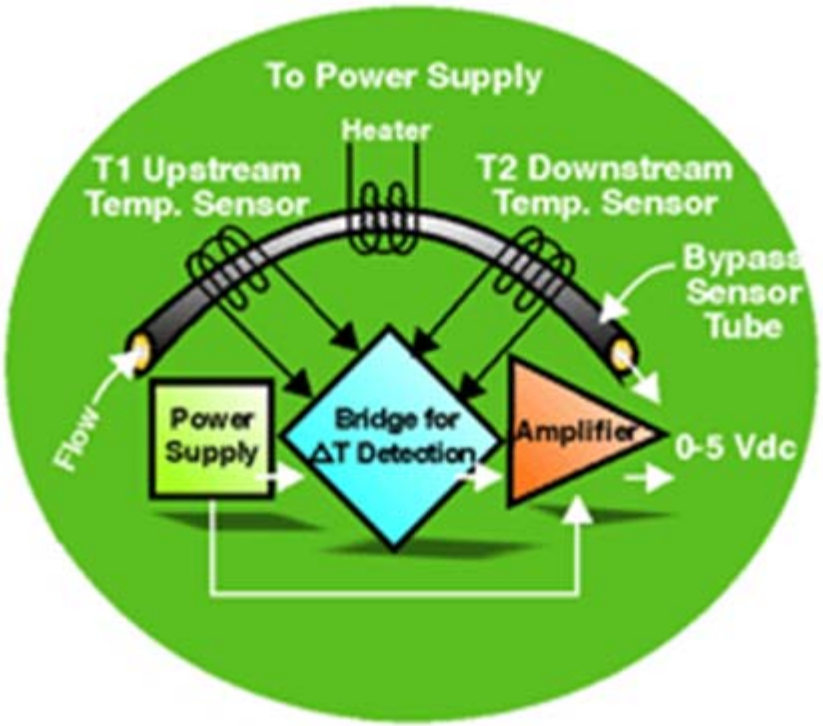

Ultrasonic flow meters

- Ultrasound is emitted to small particles in the flow (dust or other)
- Reflections of the sound is frequency shifted by the Doppler effect
- The frequency change is proportional to the particles velocity (volume flow meter)

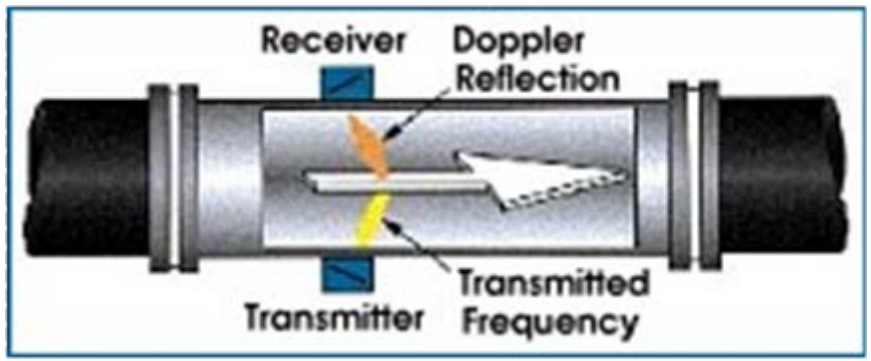

Inductive flow meters

A **magnetic flowmeter** is based upon Faraday's Law:

The voltage induced across any conductor as it moves at right angles through a magnetic field is proportional to the velocity of that conductor.

E is proportional to V x B x D where:

E = The voltage generated in a conductor
V = The velocity of the conductor
B = The magnetic field strength
D = The length of the conductor

N.B: electric conductivity is required

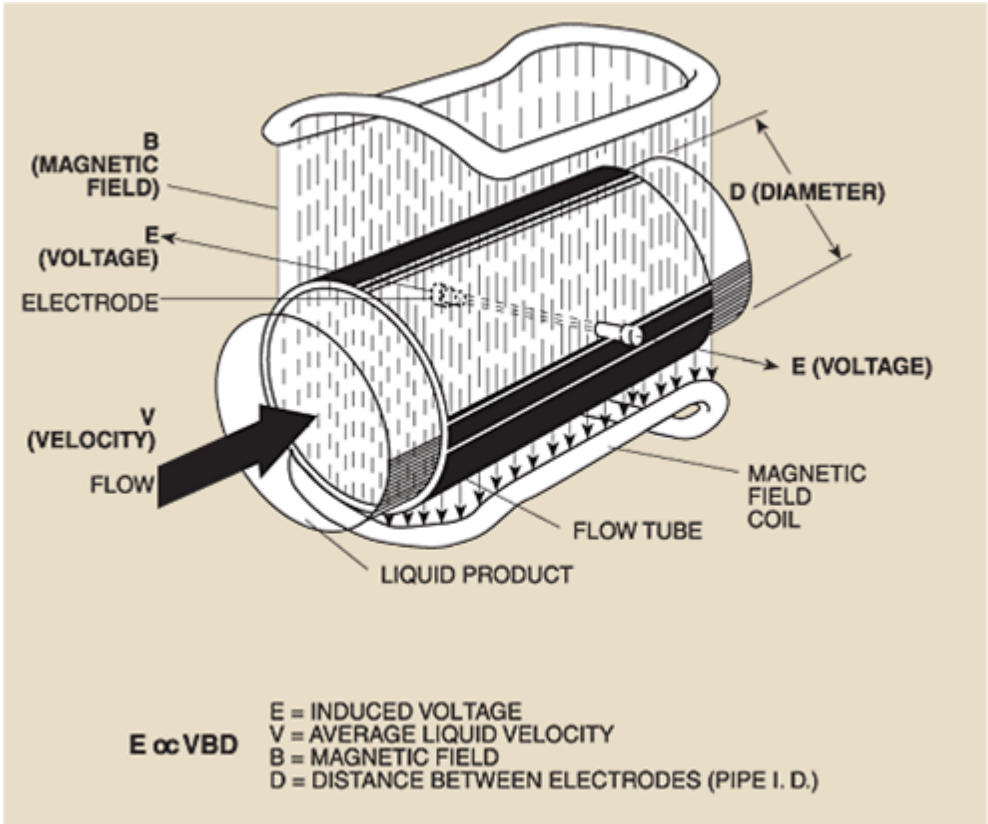

Temperature measurements

Thermocouples:

- The basis established by Thomas Johann Seebeck in 1821
- A conductor generates a voltage when subjected to a temperature gradient
- To measure this voltage, one must use a second conductor material which generates a different voltage under the same temperature gradient

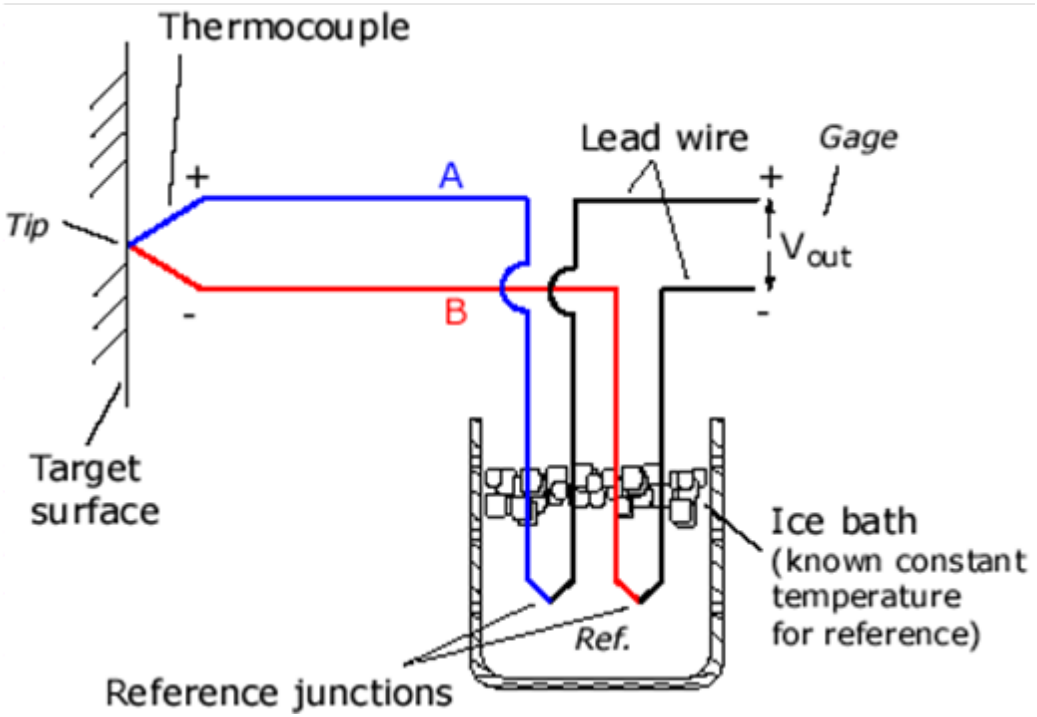

Pressure sensing

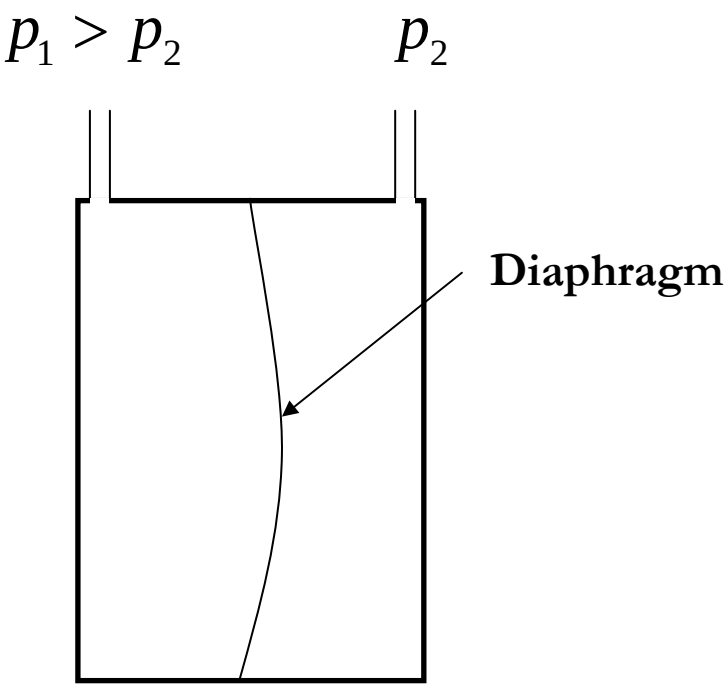

p_2 may be the atmosphere, a static pressure tap or a known reference pressure

The strain of the diaphragm (or it's deflection) may be measured by a number of electric methods

Pressure sensing

Piezoresistive Strain Gage

Uses the piezoresistive effect of bonded or formed strain gauges to detect strain due to applied pressure.

Capacitive

Uses a diaghragm and pressure cavity to create a variable capacitor to detect strain due to applied pressure.

Magnetic

Measures the displacement of a diaphragm by means of changes in inductance (reluctance), LVDT, Hall Effect, or by eddy current principal.

Piezoelectric

Uses the piezoelectric effect in certain materials such as quartz to measure the strain upon the sensing mechanism due to pressure.

Potentiometric

Uses the motion of a wiper along a resistive mechanism to detect the strain caused by applied pressure.

Point measurements

Properties of measuring object

- 3D, highly instationary (periodic) flow
- Potentially very high velocities (Supersonic)
- Large temperature differences
- Low accessibility (difficult to probe between rotors)
- Low turbulence levels in most of the domain
- Very high turbulence in BL and wakes

Point Measurements

- Conventional or non-optical
  - Static Pressure Measurements
  - Total Pressure Measurements
    - **Multy hole probes**
  - Total Temperature
  - Hot Wire Anemometry (HWA)
- Optical techniques for Velocity Measurements
  - Laser Two Focous (L2F)
  - Laser Doppler Anemometry (LDA)
  - Particle Image velocimetry (PIV)

Static and total pressure

Prandtl or Pitot tube

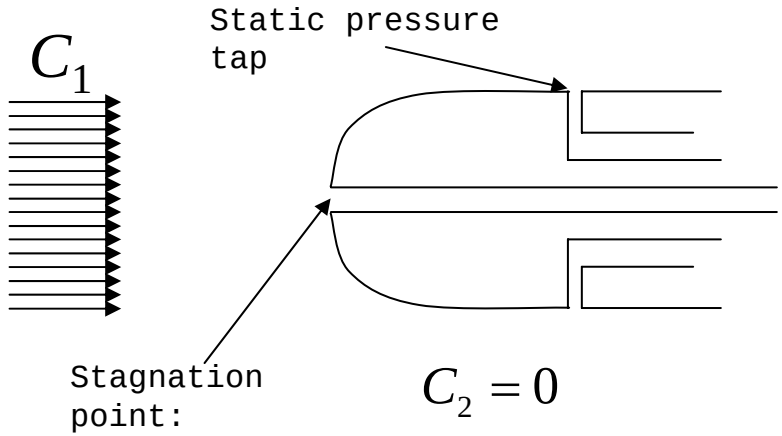

Apply the Bernoulli equation from free stream to stagnation point:

$$P_2 - P_1 = \frac{\rho C_1^2}{2} - \frac{\rho C_2^2}{2} = \frac{\rho C_1^2}{2} \quad \text{or} \quad P_2 = \frac{\rho C_1^2}{2} + P_1$$

We can also define a stagnation or total pressure:

$$P_{01} = P_1 + \frac{\rho C_1^2}{2} \left(= P_{02}\right) \quad \text{or}$$

Total pressure = Static pressure + dynamic pressure

Static pressure

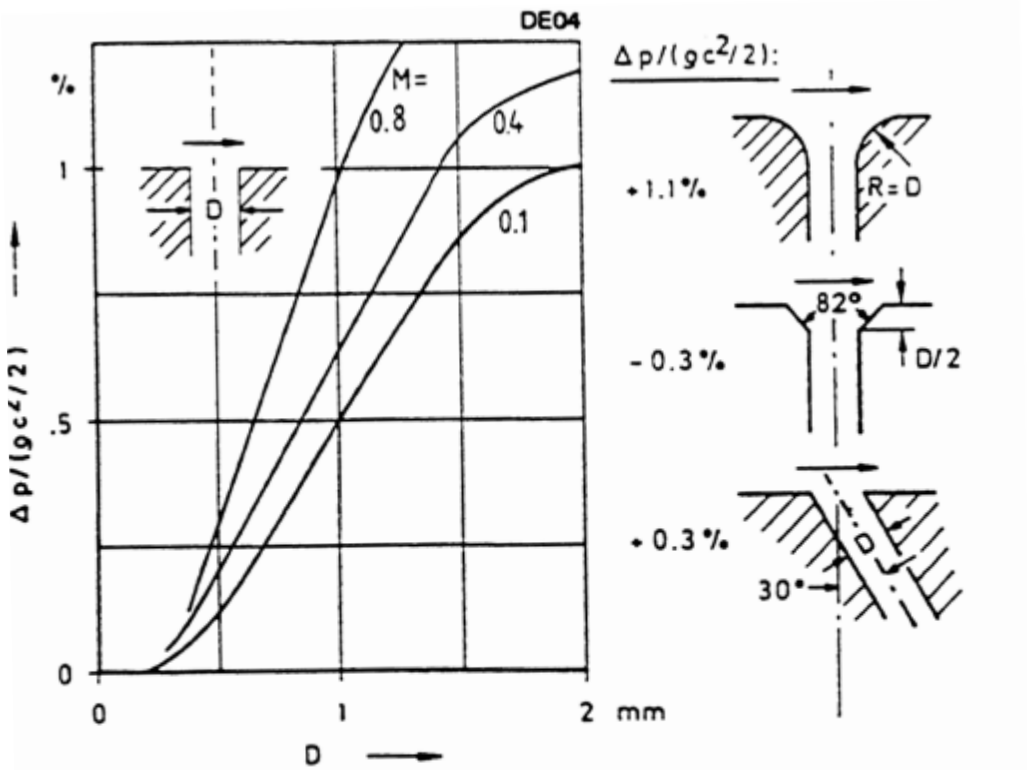

Figure 4. Influence of Hole Dimensions, Mach Number, and Orifice Edge Form on Static Pressure Measurements (Error, Δp, in Percent of Dynamic Head)

Total Pressure and Temperature

Pitot or Prandtl tube

Sensitive to direction

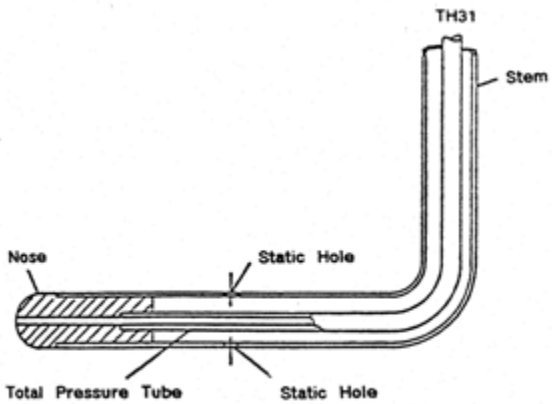

Shrouded Probes

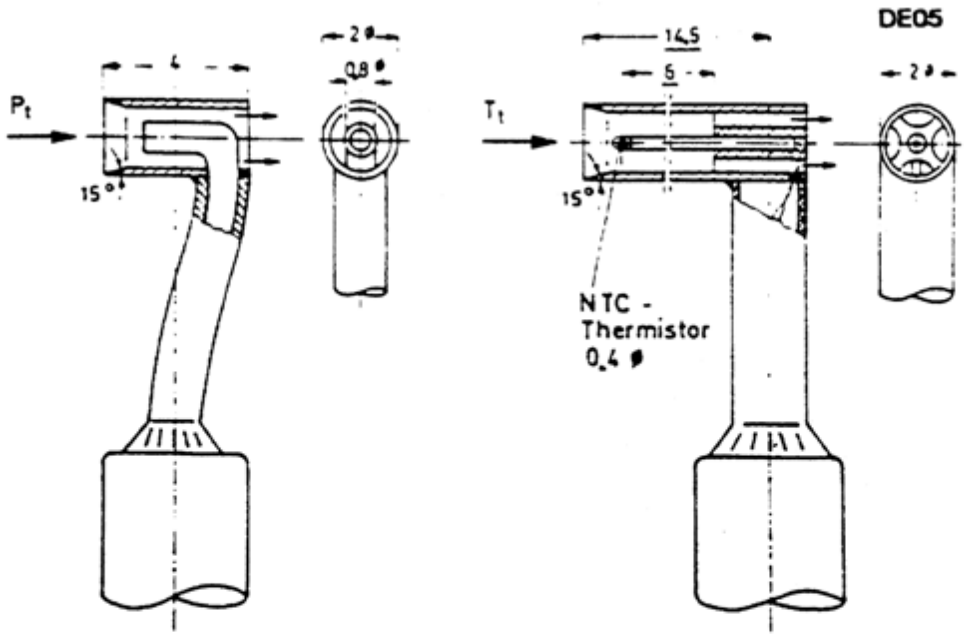

Figure 5. Conventional Time-Averaging Probes of the Kiel Type: Left-Total Pressure Probe, Right-Total Temperature Probe (Dimensions in mm)

Ludwig Prandtl 1875-1953

Ludwig Prandtl, born at Freising, Bavaria on February 4, 1875, was a German Physicist famous for his work in aeronautics. He qualified at Munchen in 1900 with a thesis on elastic stability and held the position of Professor of Applied Mechanics at Gottingen for forty-nine years (from 1904 until his death there on August 15, 1953).

In 1925, Prandtl became the Director of the Kaiser Wilhelm Institute for Fluid Mechanics. His discovery in 1904 of the Boundary Layer which adjoins the surface of a body moving in a fluid led to an understanding of skin friction drag and of the way in which streamlining reduces the drag of airplane wings and other moving bodies. His work on wing theory, published in 1918 - 1919, followed that of F.W. Lanchester (1902-1907), but was carried out independently and elucidated the flow over airplane wings of finite span. Prandtl's work and decisive advances in boundary layer and wing theories became the basic material of aeronautics. He also made important contributions to the theories of supersonic flow and of turbulence, and contributed much to the development of wind tunnels and other aerodynamic equipment. In addition, he devised the soap-film analogy for the torsion of non-circular sections and wrote on the theory of plasticity and of meteorology.

Total Pressure, multy hole

Cobra Probe

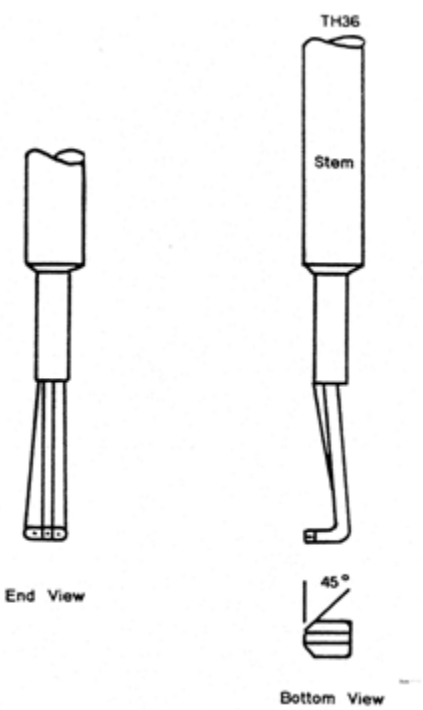

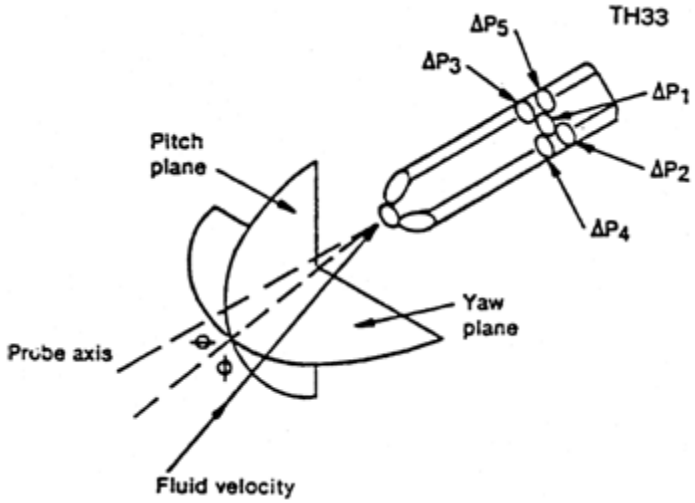

5 Hole Probe

Yaw Probe

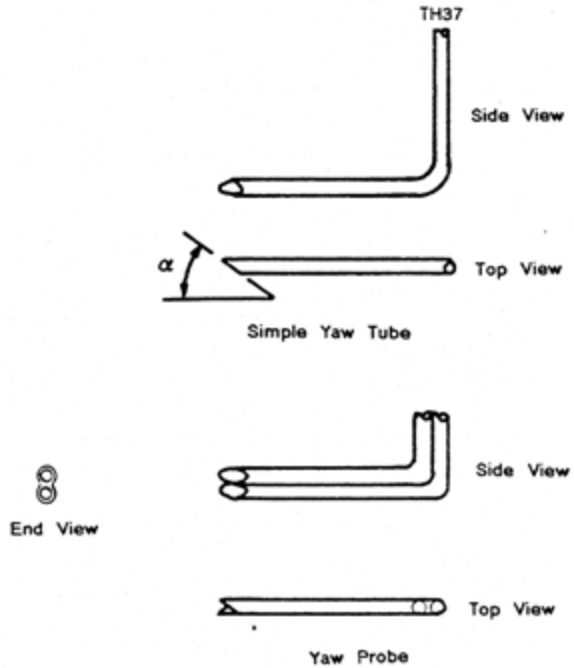

5 Hole Probes, Calibration

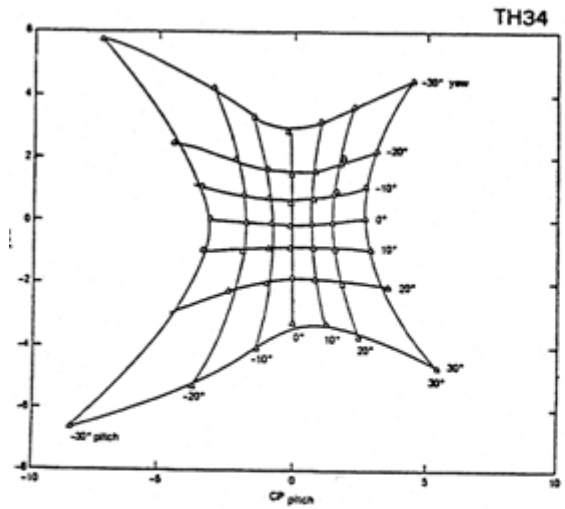

ure II-4. Five-Point Probe Calibration in Water, CP_{yaw} vs. CP_{pitch}

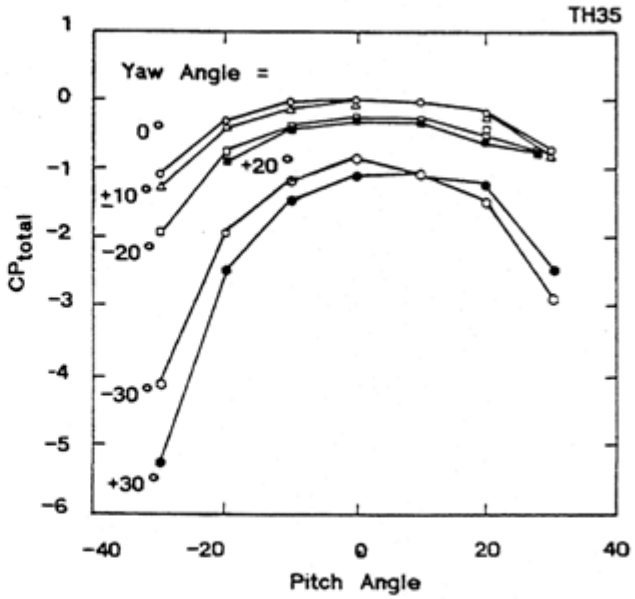

Figure II-5. Five-Point Probe Calibration in Water, CP_{total} vs. Pitch Angle

The inherent unsteadiness of the flow within turbomachines

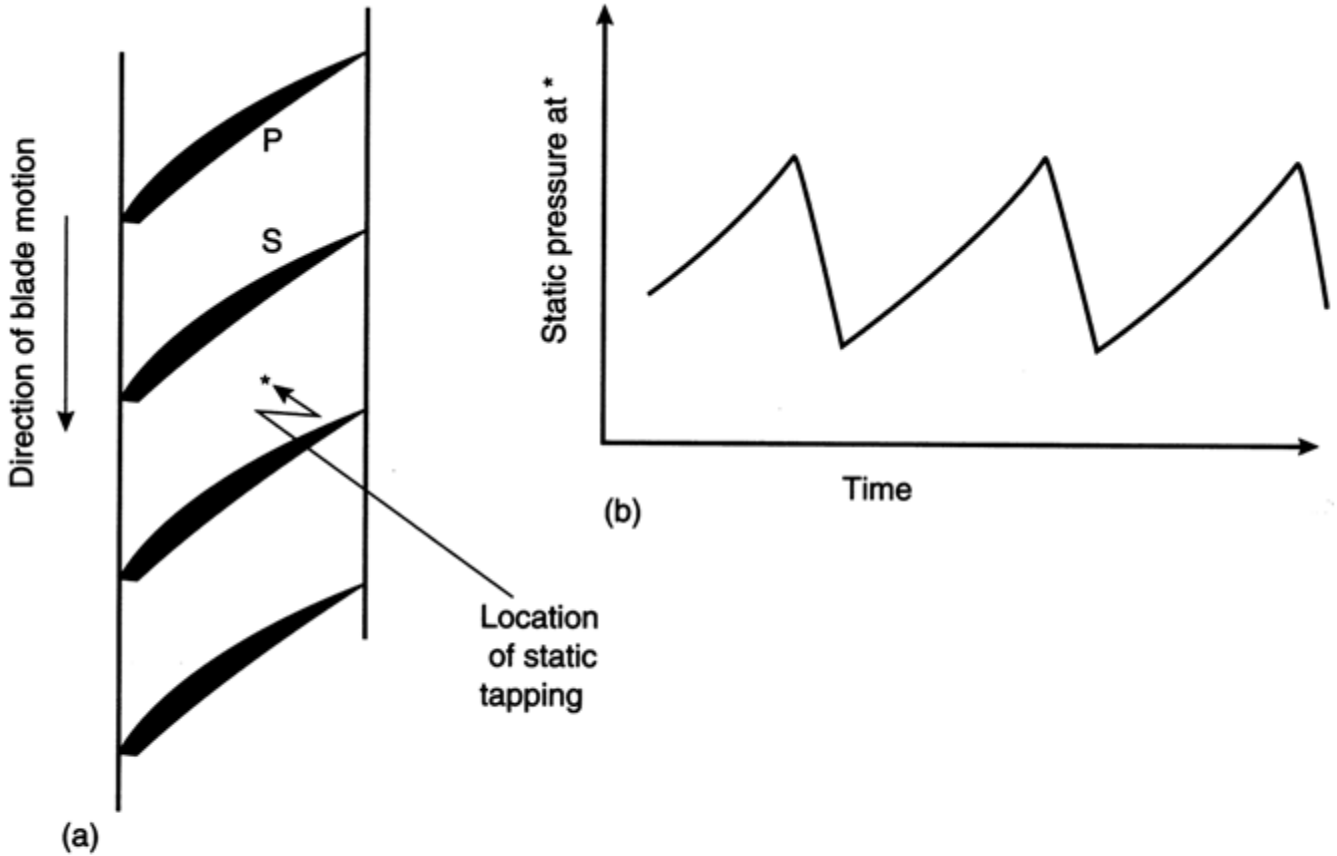

FIG. 1.12. Measuring unsteady pressure field of an axial compressor rotor. (a) Pressure is measured at point ∗ on the casing. (b) Fluctuating pressure measured at point ∗.

Hot Wire Anemometry (HWA)

- The heat transfer from a thin (one micron), electrically heated wire can be used to determine velocity.
- The resistance of the wire is temperature dependent. Within a small temperature range it can be assumed linear: $R = R_0+\alpha\ R_0(T_m-T_0)$ where R_0 is the resistance at a reference temperature T_0 and T_m is the mean wire temperature.
- The thermal power induced in the wire is balanced by heat transfer to the surrounding fluid, $I^2R=h\pi DL(T_m-T_0)$, where h is the heat transfer coefficient and D and L the diameter and length of the wire, respectively.

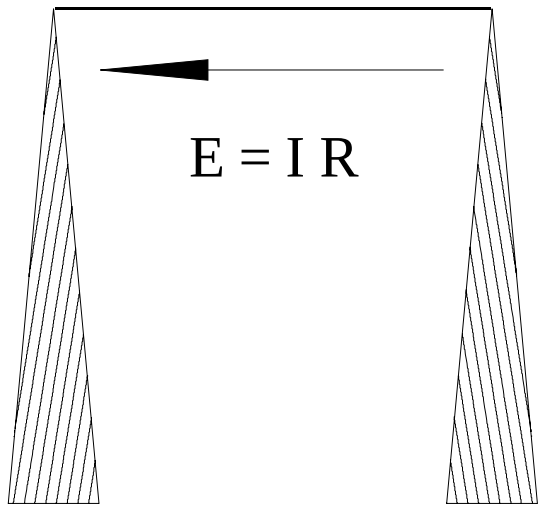

Constant Temperature Anemometry (CTA)

- The wire is often placed in a Whetstone bridge. If the output from the bridge is amplified and fed back to the bridge, the resistance of the probe, and thus the temperature, will be held constant.
- This prevents the temperature of the wire to become excessive at low velocities.

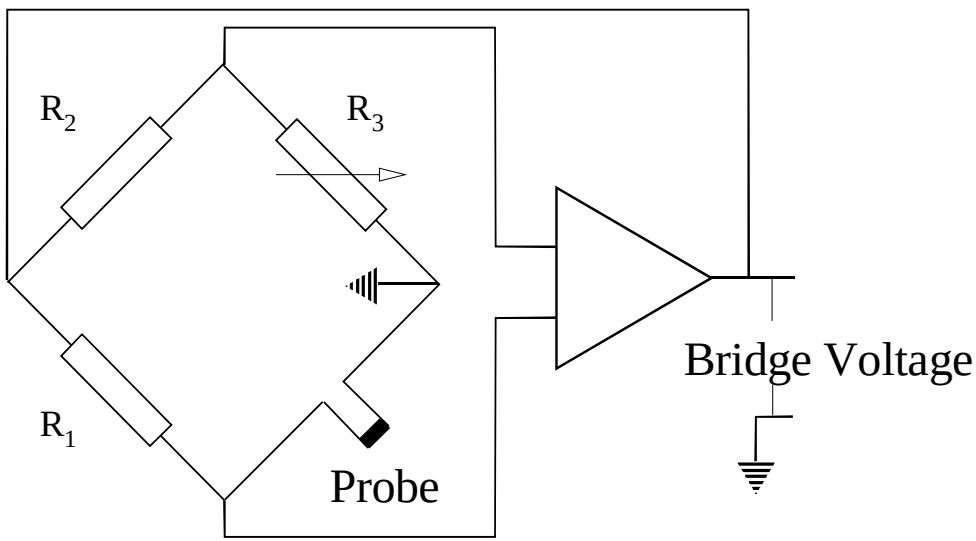

Constant Temperature Anemometry (CTA)

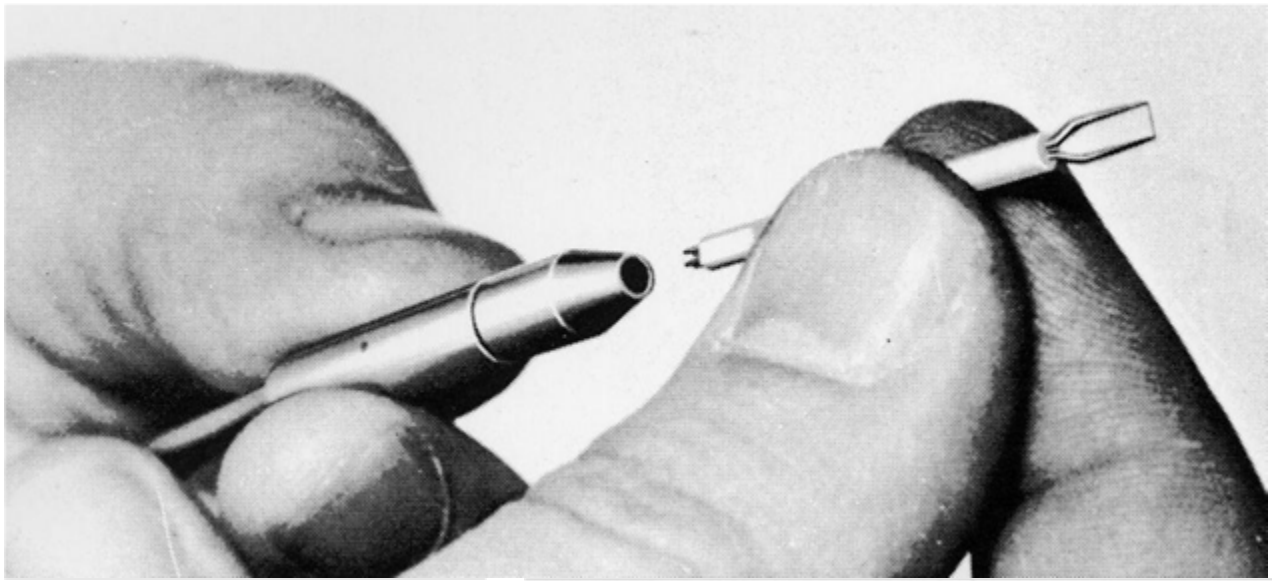

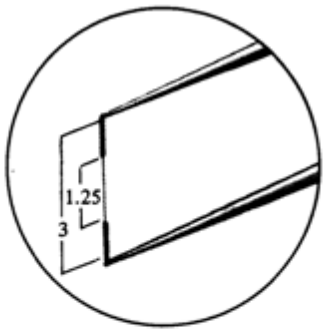

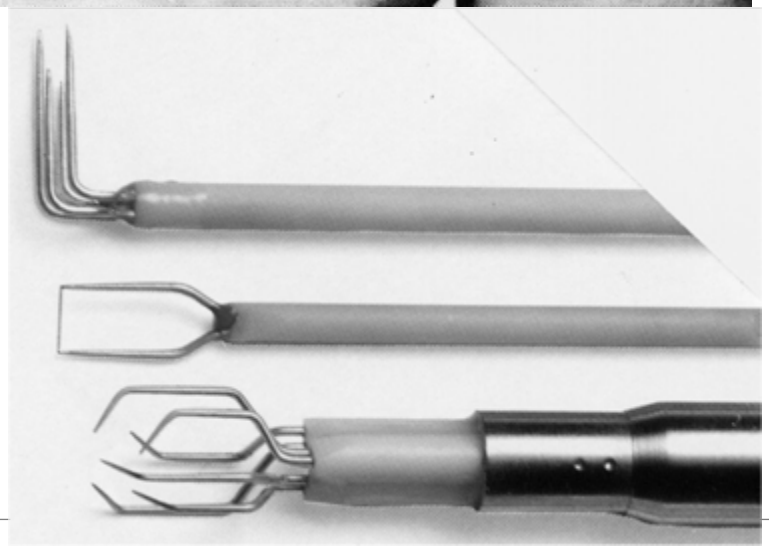

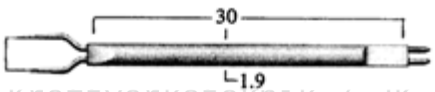

Characteristics of LDA (according to Dantec)

- Invented by Yeh and Cummins in 1964
- Velocity measurements in Fluid Dynamics (gas, liquid)
- Up to 3 velocity components
- Non-intrusive measurements (optical technique)
- Absolute measurement technique (no calibration required)
- Very high accuracy
- Very high spatial resolution due to small measurement volume
- Tracer particles are required

LDA - Fringe Model

- Focused Laser beams intersect and form the measurement volume
- Plane wave fronts: beam waist in the plane of intersection
- Interference in the plane of intersection
- Pattern of bright and dark stripes/planes: Fringes

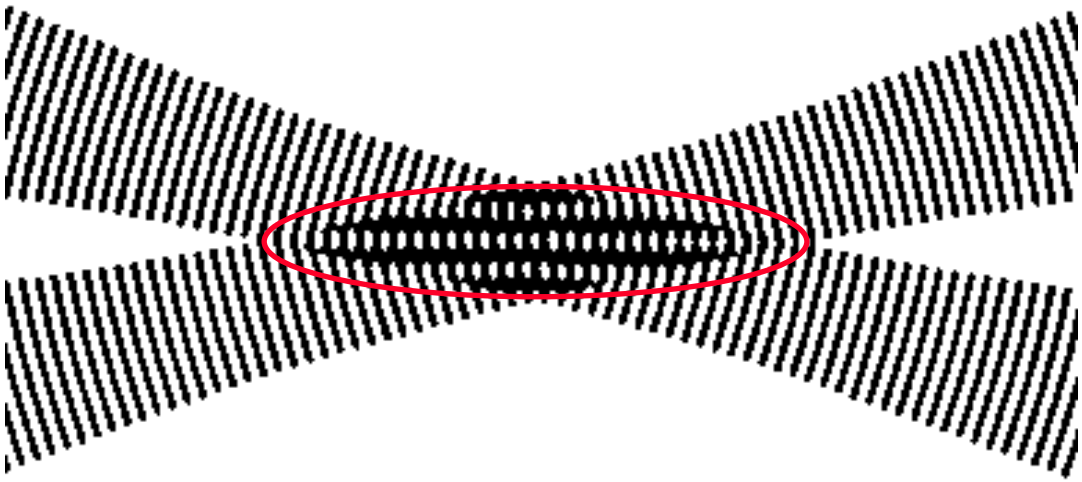

LDA-measuring volume

$$l_m = \frac{4\,\lambda\,f}{\pi\,D_{e^{-2}}\,\sin\kappa}$$

$$D_m = \frac{4\,\lambda\,f}{\pi\,D_{e^{-2}}\,\cos\kappa}$$

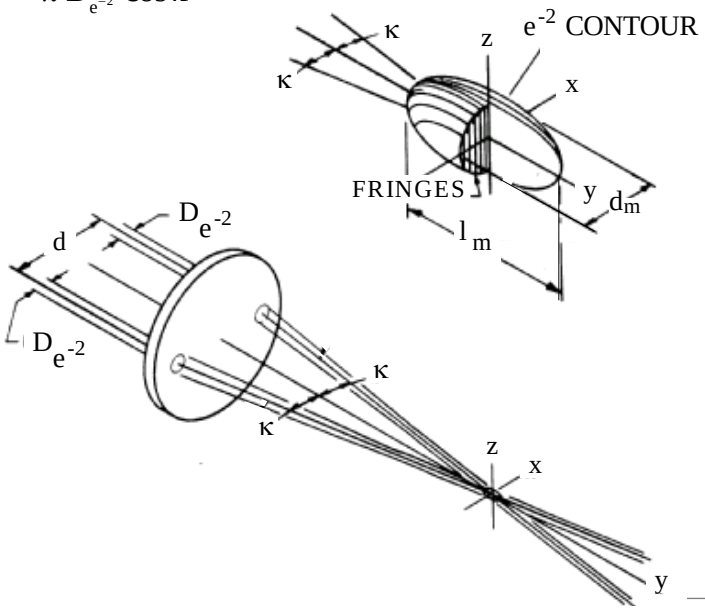

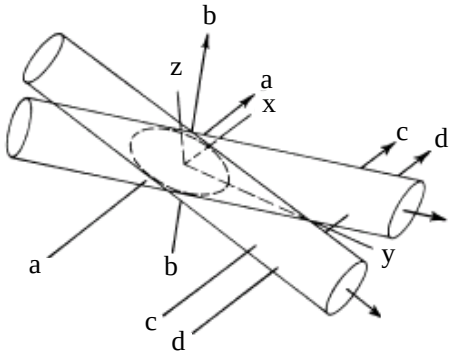

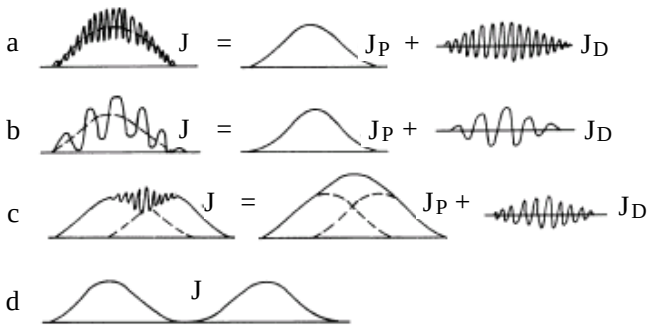

Laser Two Focus

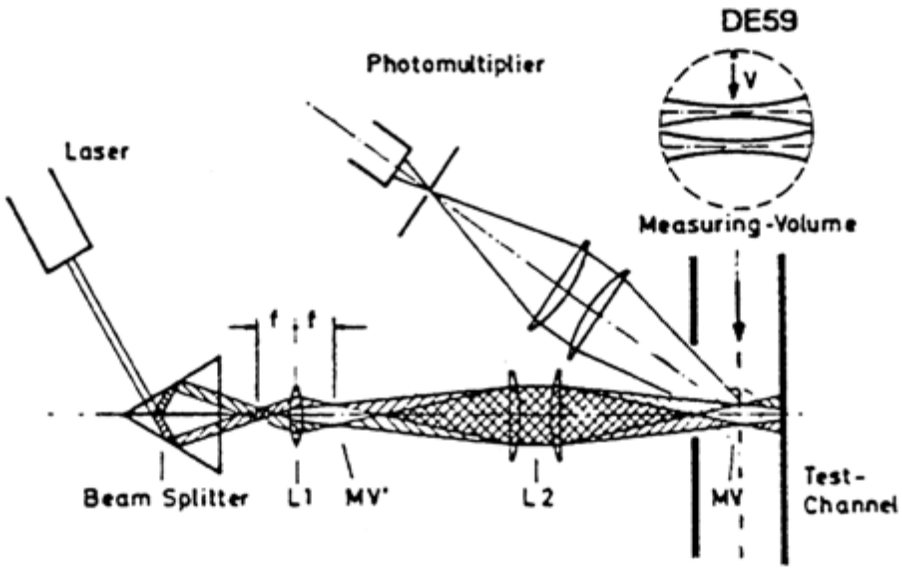

Figure 60. Scheme of the Laser 2-Focus Velocimeter (L2F)

Laser Two Focus

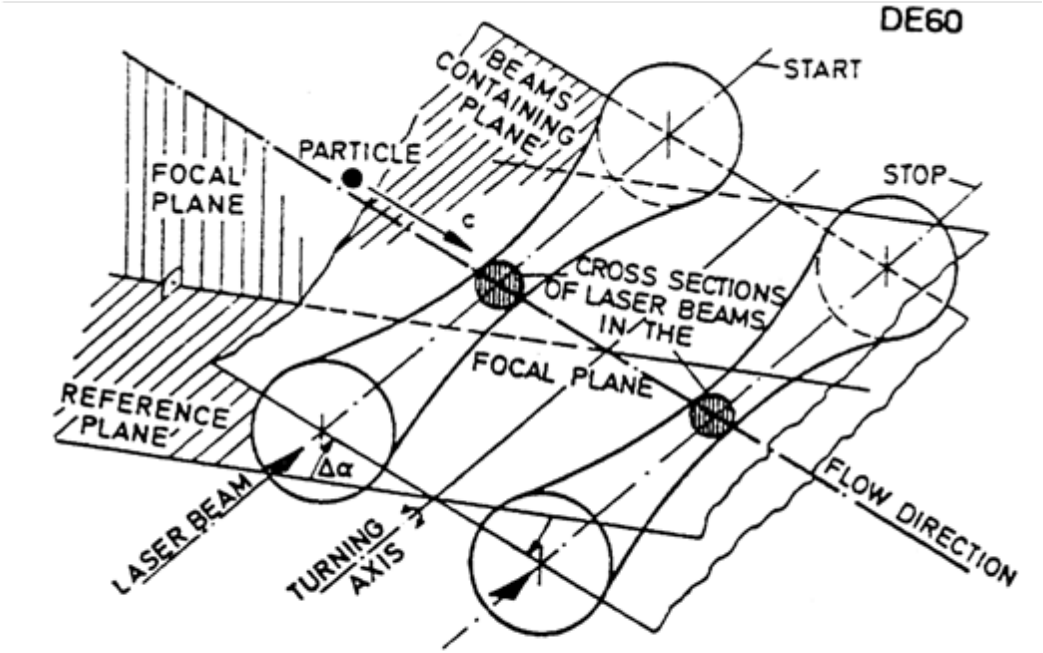

Figure 61. Principal Sketch of the L2F Measuring Volume

PIV measurements

- PIV is a fairly new technique, capable of simultaneous velocity measurements at many points in a plane. This gives information on large scale structures, vorticity etc. which is very difficult or impossible to obtain from one-point measuring techniques.
- PIV involves the illumination of a plane of the flow under investigation with a thin, pulsed sheet of light. The flow is seeded with particles.
- The light scattered from the particles and from successive pulses are being recorded either on film or a CCD array, forming a multiple exposure of each particle image. If the time between the pulses is known, velocity can be determined as the ratio of the particle displacement and the elapsed time:

$$\mathbf{u} = \Delta\mathbf{x} / \Delta t$$

PIV

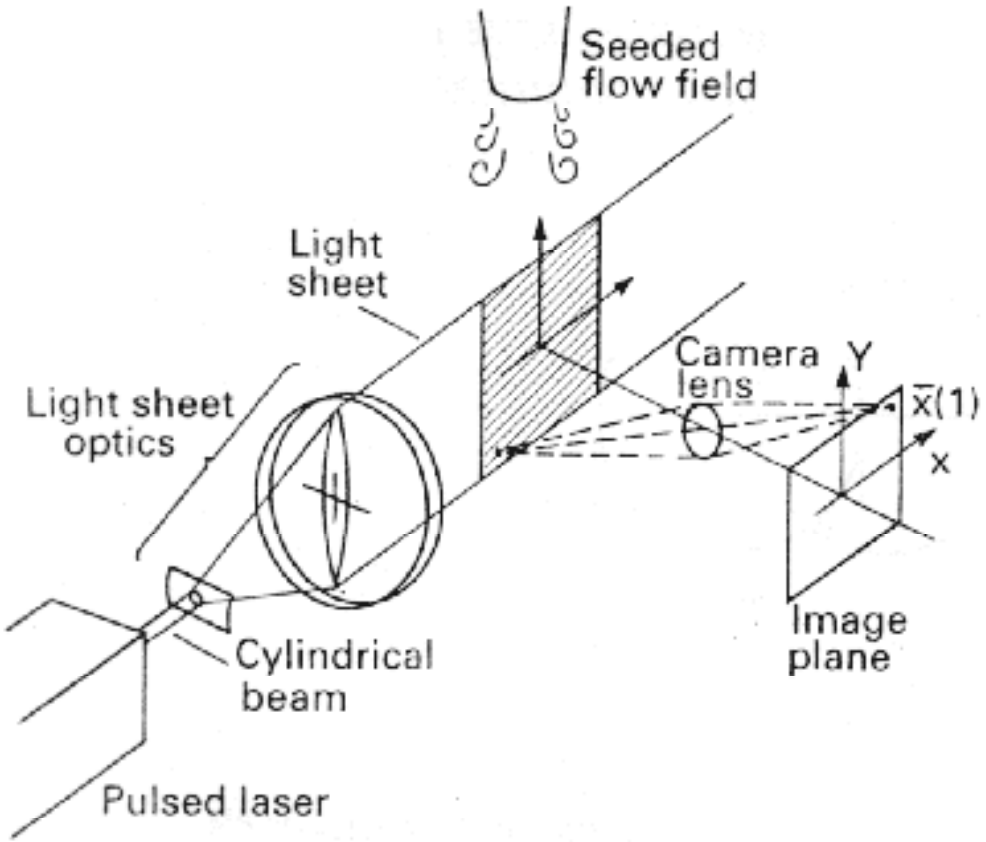
Seeded
flow field
Light
sheet
Light sheet
optics
Camera
lens
Y
x̄(1)
x
Cylindrical
beam
Image
plane
Pulsed laser

PIV measurements, illumination

- Two, or more, separate light pulses can be obtained by chopping a continuous laser or from pulsed lasers.
- The limited pulse energies obtained from continuous lasers limits their applicability to low velocity flows or flows where large seeding particles can be used (i.e. liquid flows).
- The low repetition rate of most pulsed lasers makes the use of two lasers advantageous.

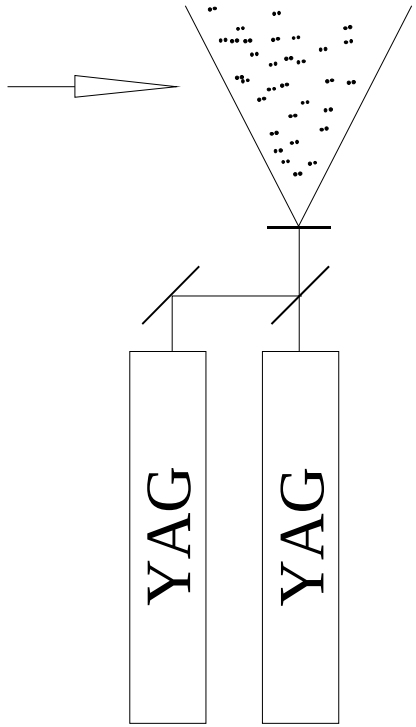

Two frequency doubled YAG Lasers aligned to one double pulsed laser sheet

PIV measurements, recording

- Film or CCD-cameras
- Cross- or Auto-correlation
  - i.e. both particle images on the same frame or on separate frames.
- CCD-camera requirement:
  - A many pixels as possible
  - 2k by 2k available, 4k, by 4k coming

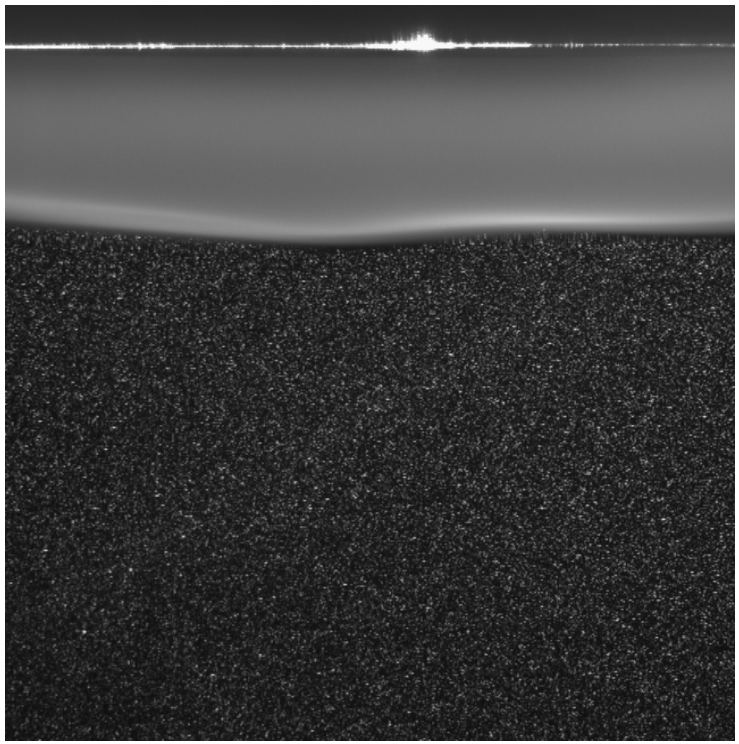

High seeding density in laminar flame

PIV measurements, analyses

Low seeding density: (Number of seeding particles per unit volume)

Each particle image pair can be identified.
This is called particle tracking.

High seeding density: (PIV)

Small sub-regions of the image, containing many particle image pairs, are processed to obtain one velocity vector.

PIV measurements, analyses

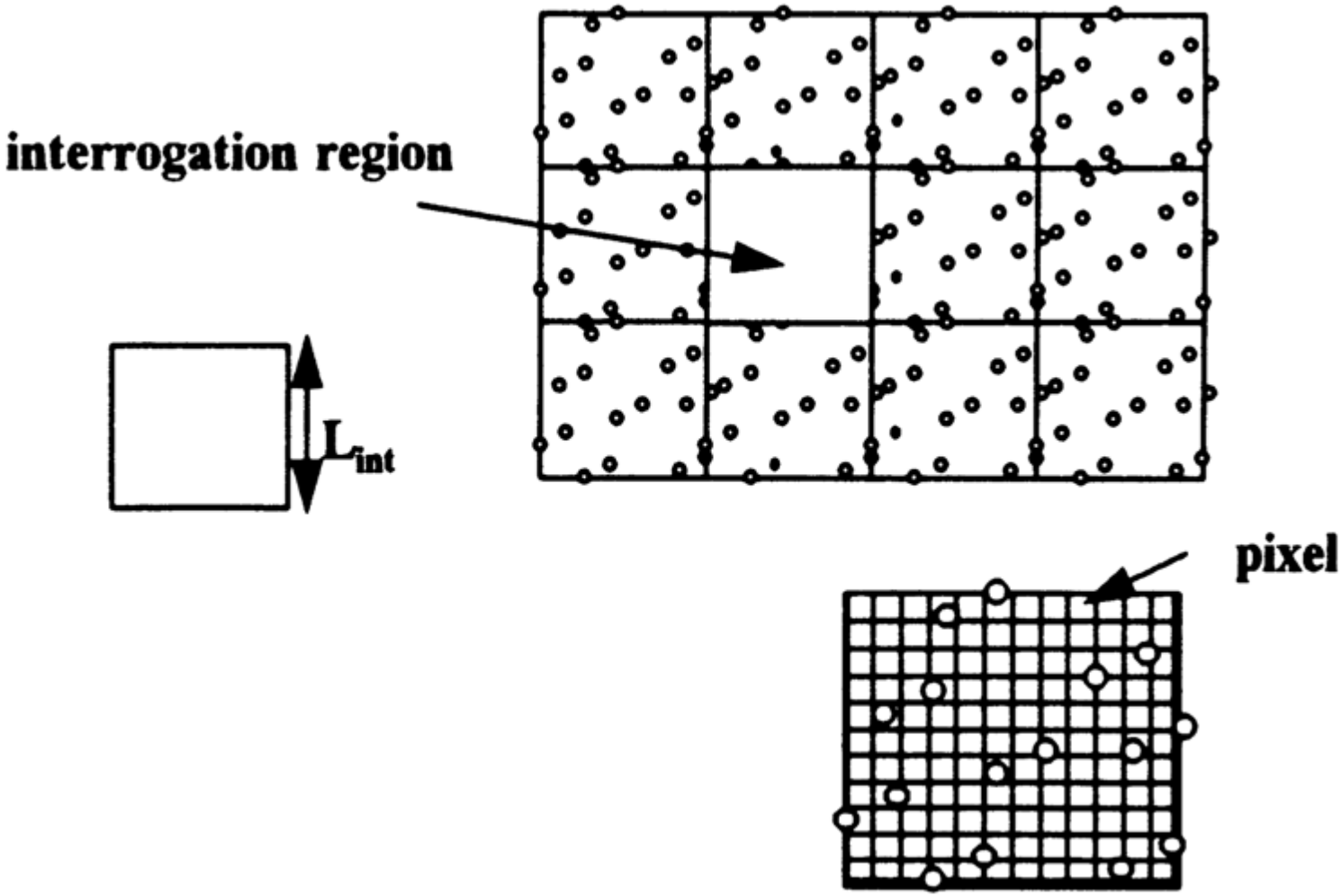

PIV measurements, analyses

Cross correlation between $I_1(\mathbf{x})$ and $I_2(\mathbf{x})$

$$R(\mathbf{s}) = \int_{A_I} I_1(\mathbf{x})\, I_2(\mathbf{x}+\mathbf{s})\, d\mathbf{x}$$

s is a two dimensional displacement vector

A_I is the interrogation area

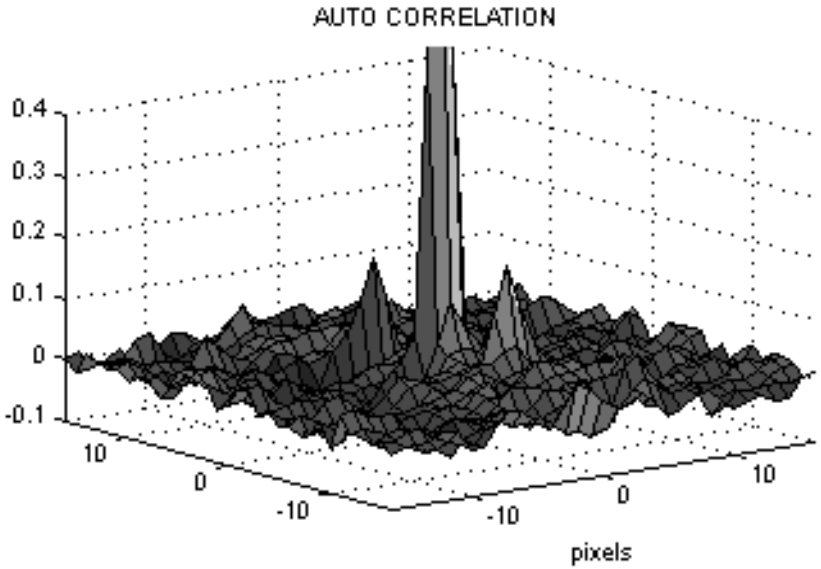
AUTO CORRELATION
0.4
0.3
0.2
0.1
0
-0.1
10
0
-10
-10
0
10
pixels

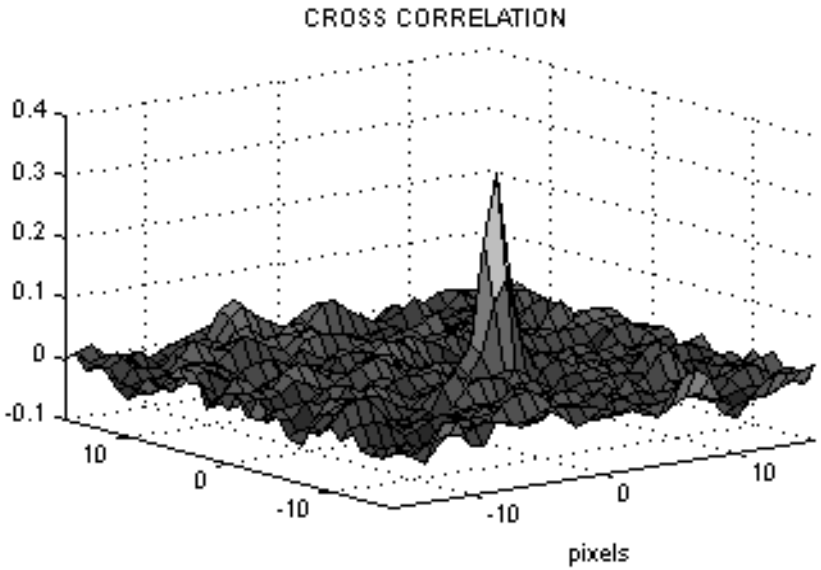
CROSS CORRELATION
0.4
0.3
0.2
0.1
0
-0.1
10
0
-10
-10
0
10
pixels

PIV, sample of evaluation

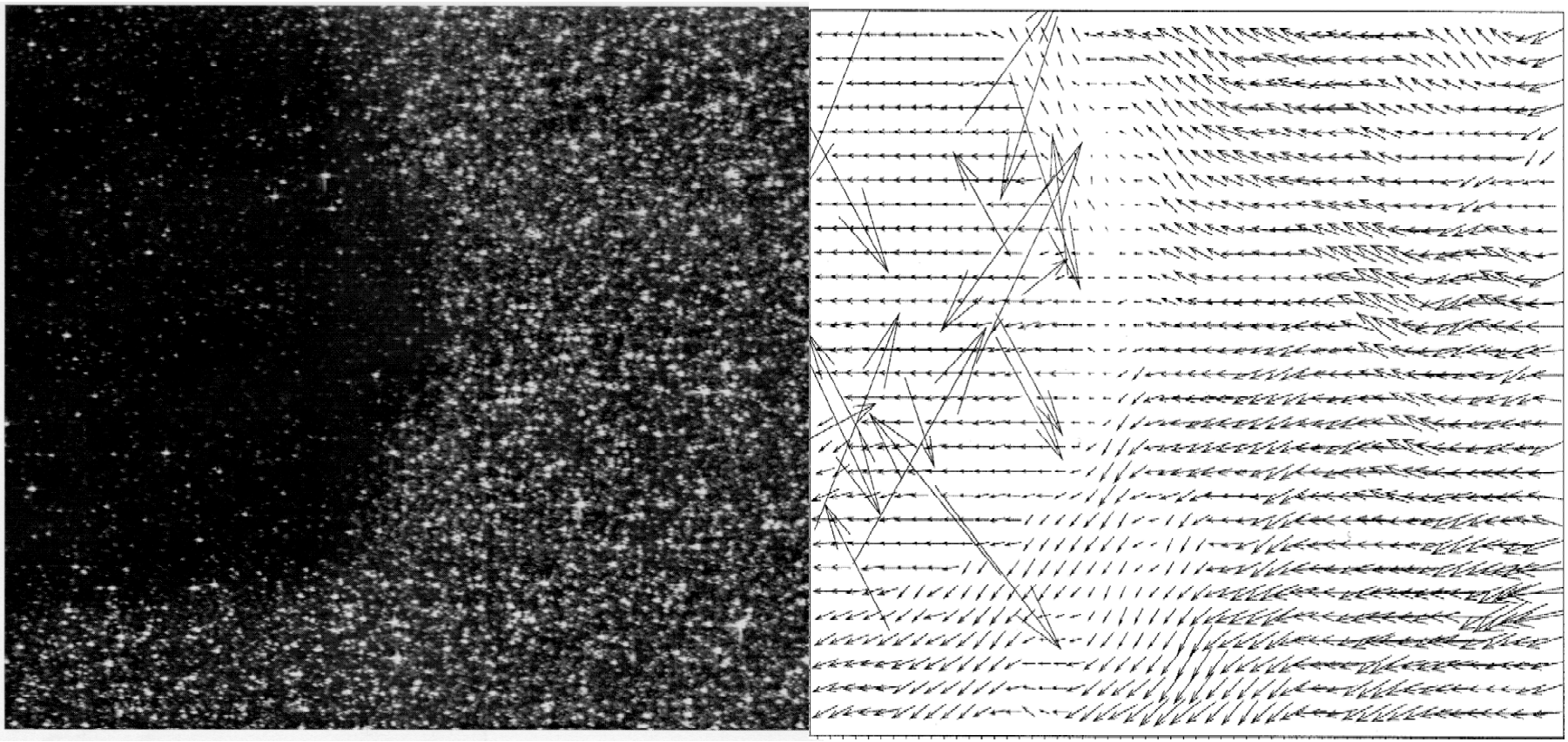

Comparison of techniques

	LDA	**PIV**	**HWA**
Velocity range	0.1 mm/s – 300 m/s		0.2 – 150 m/s
Measuring Volume	D = 0.05, L = 0.5 mm	2 by 2 by 0.5 mm	L = 0.5 mm
Freq. response	O(10 000) Hz	O(10) Hz	O(100 000) Hz
Calibration	Yes	No	No
Sensitivity to other than velocity	Low (ref. Index)	Low (ref. Index)	Large (temperature, concentrations…)
Continuous Signal	Sometimes	Seldom	Always
Noise	High	High	Low
Turbulence intensity	No limitation	Some limitation	< 20%
Price	O(1 000 000) SEK	O(1 000 000) SEK	O(50 000) SEK
Required Knowledge	High	medium	Low

References, experiments

- **R. J. Goldstein, *"Fluid Mechanics Measurements"*, Hemisphere Publishing, 1983.**
- **A. V. Johansson & P. H. Alfredsson, *"Experimentella metoder inom strömningsmekaniken"*, Inst. För Mekanik, KTH.**
- **F. Durst, A. Melling and J. H. Whitelaw, *"Principals and Practice of Laser Doppler Anemometry"*, 1984**
- **R. J. Adrian, *"Particle-imaging techniques for experimental fluid mechnics"*, Ann. Rev. Fluid Mech., 1991.**

Sample of LDA-measurements

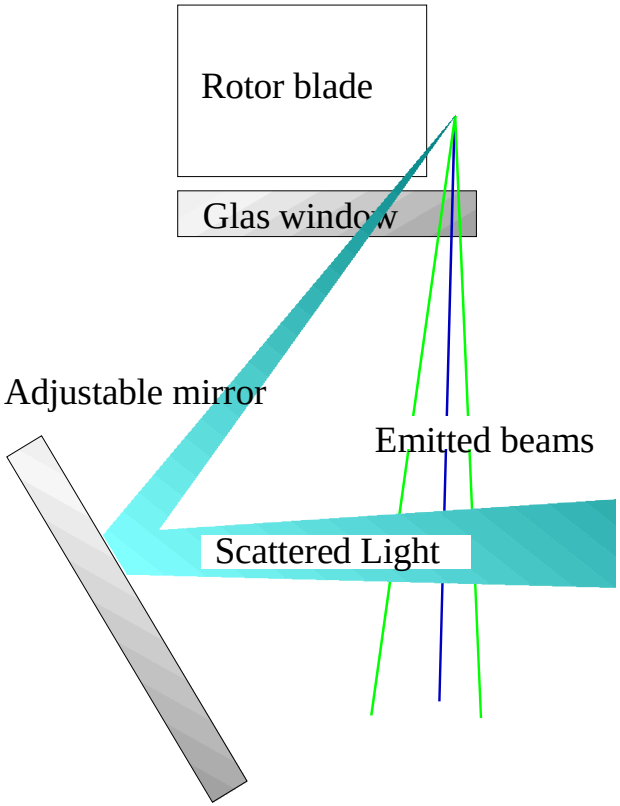

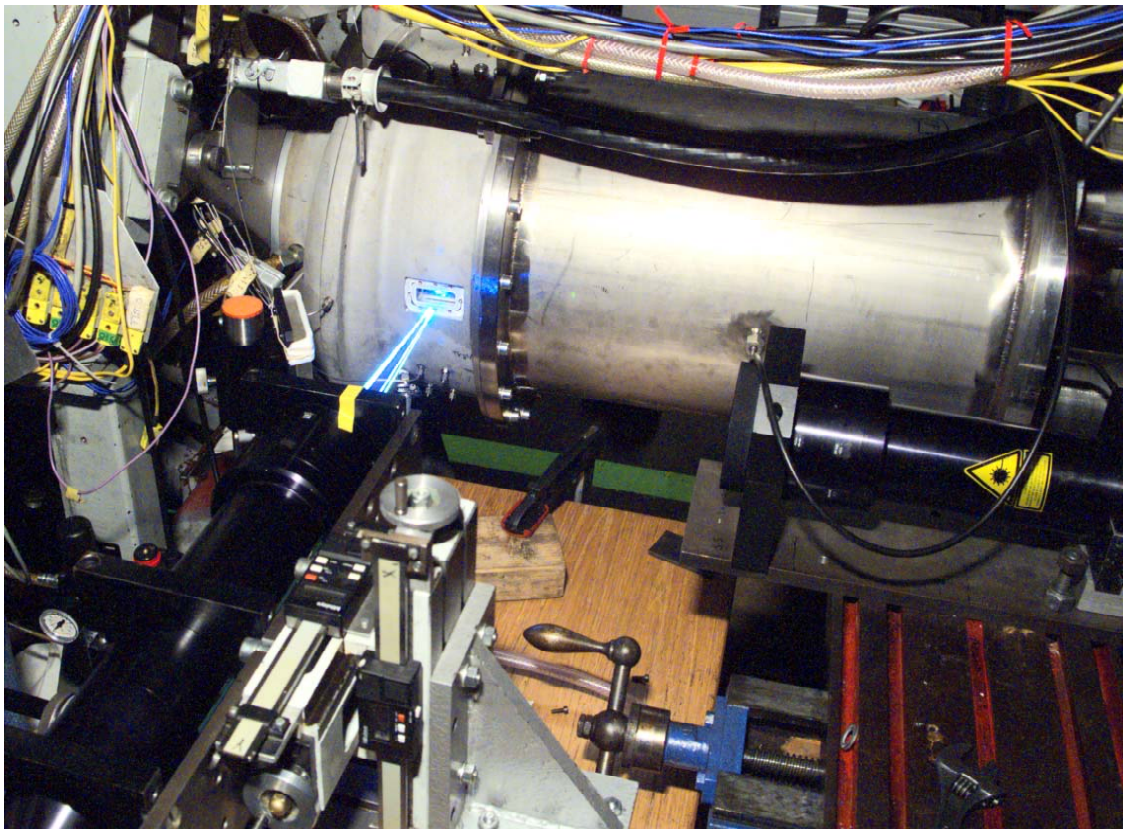

Axial velocity sorted into 10 bins

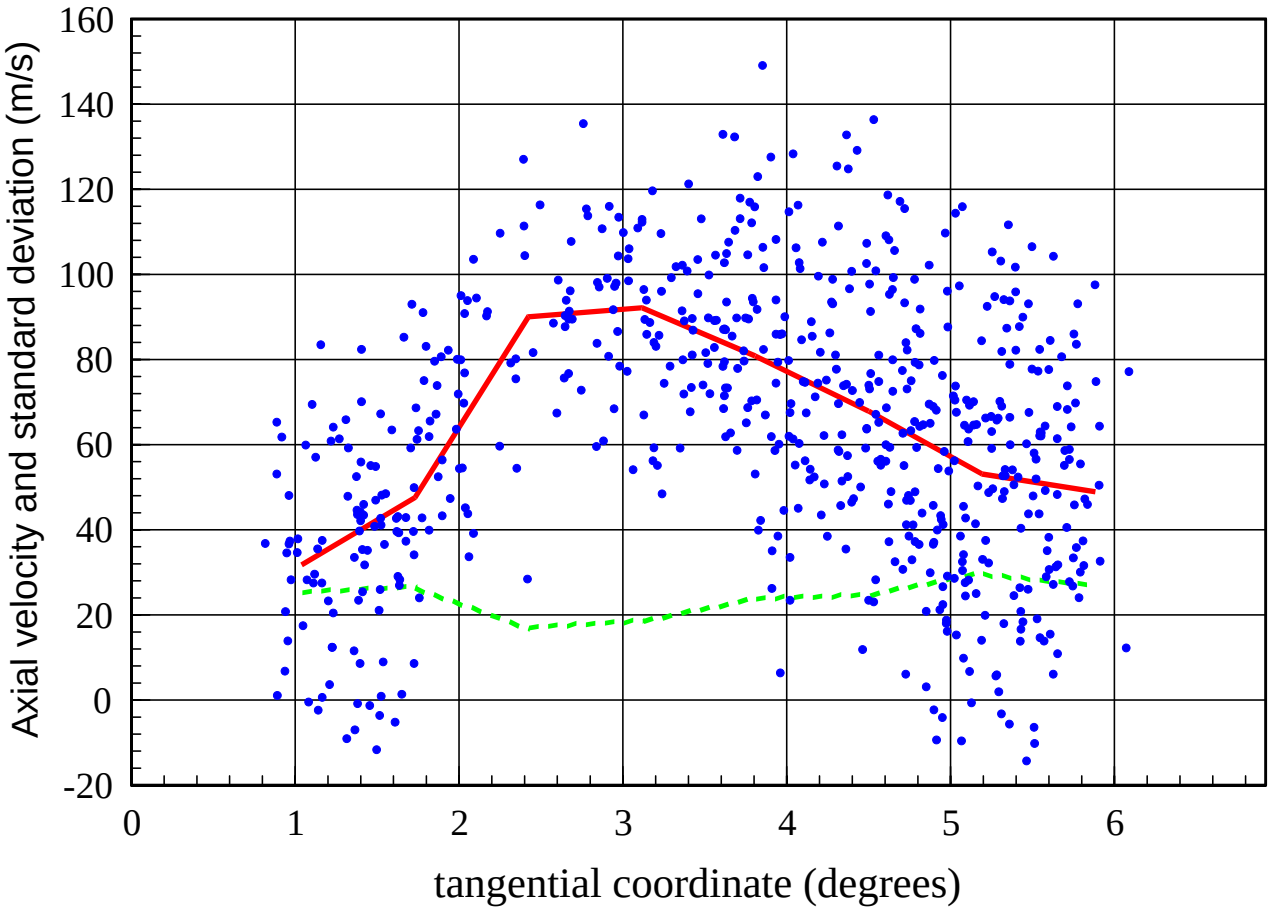

radial position: 7 mm from inner window surface
axial position: 2.3 mm behind rotor blades

Axial velocities in the radial-tangential plane

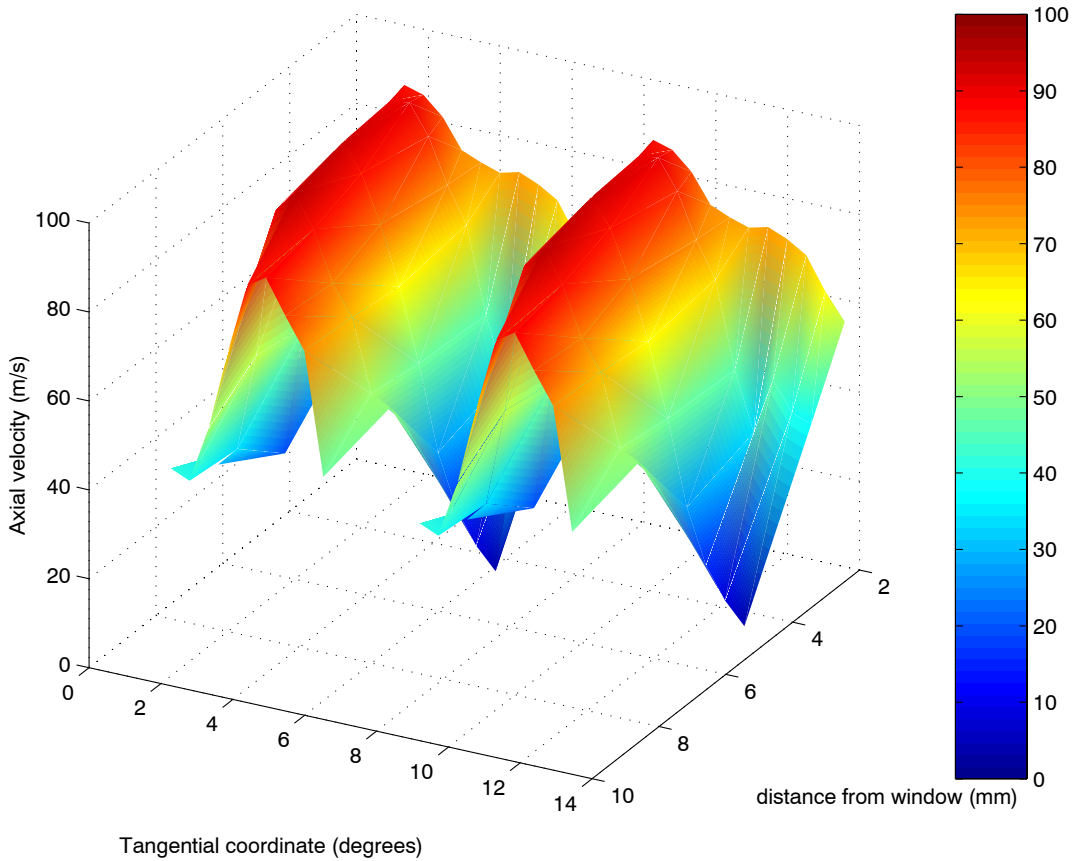

Airfoils: NACA 4-digit

The NACA four-digit wing sections define the profile by:

- **One digit describing maximum camber as percentage of the chord.**
- **One digit describing the distance of maximum camber from the airfoil leading edge in tens of percents of the chord.**
- **Two digits describing maximum thickness of the airfoil as percent of the chord.**

Example, the NACA 2412 airfoil has a maximum camber of 2% located 40% (0.4 chords) from the leading edge with a maximum thickness of 12% of the chord.

Four-digit series airfoils by default have maximum thickness at 30% of the chord (0.3 chords) from the leading edge.

Airfoils: NACA 4-digit

$$y = \frac{t}{0.20}\left[0.2969 \times \sqrt{\frac{x}{c}} - 0.1260\left(\frac{x}{c}\right) - 0.3516\left(\frac{x}{c}\right)^2 + 0.2843\left(\frac{x}{c}\right)^3 - 0.1015\left(\frac{x}{c}\right)^4\right],$$

- **c is the chord length**
- **x is the position along the chord from 0 to c,**
- **y is the half thickness at a given value of x (centerline to surface)**
- **t is the maximum thickness as a fraction of the chord**

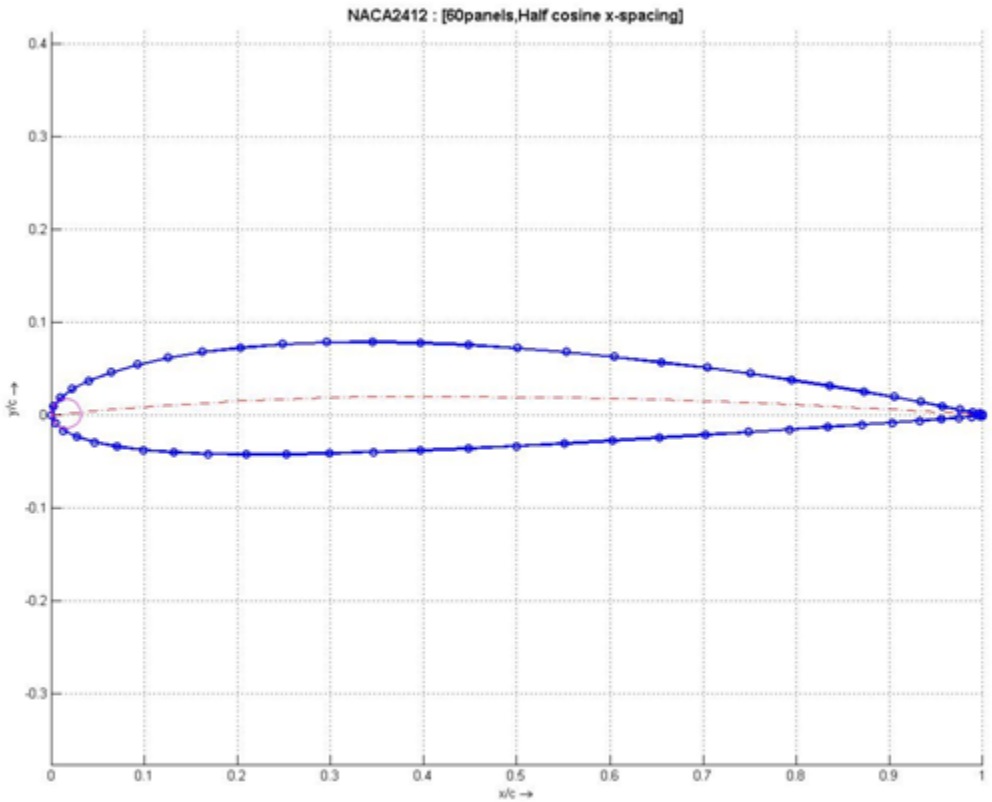

Death by PowerPoint